NBS TECHNICAL NOTE **1191**

U.S. DEPARTMENT OF COMMERCE/National Bureau of Standards

Electrical Parameters in 60-Hz Biological Exposure Systems and Their Measurement: A Primer

NATIONAL BUREAU OF STANDARDS

The National Bureau of Standards[1] was established by an act of Congress on March 3, 1901. The Bureau's overall goal is to strengthen and advance the Nation's science and technology and facilitate their effective application for public benefit. To this end, the Bureau conducts research and provides: (1) a basis for the Nation's physical measurement system, (2) scientific and technological services for industry and government, (3) a technical basis for equity in trade, and (4) technical services to promote public safety. The Bureau's technical work is performed by the National Measurement Laboratory, the National Engineering Laboratory, and the Institute for Computer Sciences and Technology.

THE NATIONAL MEASUREMENT LABORATORY provides the national system of physical and chemical and materials measurement; coordinates the system with measurement systems of other nations and furnishes essential services leading to accurate and uniform physical and chemical measurement throughout the Nation's scientific community, industry, and commerce; conducts materials research leading to improved methods of measurement, standards, and data on the properties of materials needed by industry, commerce, educational institutions, and Government; provides advisory and research services to other Government agencies; develops, produces, and distributes Standard Reference Materials; and provides calibration services. The Laboratory consists of the following centers:

Absolute Physical Quantities[2] — Radiation Research — Chemical Physics — Analytical Chemistry — Materials Science

THE NATIONAL ENGINEERING LABORATORY provides technology and technical services to the public and private sectors to address national needs and to solve national problems; conducts research in engineering and applied science in support of these efforts; builds and maintains competence in the necessary disciplines required to carry out this research and technical service; develops engineering data and measurement capabilities; provides engineering measurement traceability services; develops test methods and proposes engineering standards and code changes; develops and proposes new engineering practices; and develops and improves mechanisms to transfer results of its research to the ultimate user. The Laboratory consists of the following centers:

Applied Mathematics — Electronics and Electrical Engineering[2] — Manufacturing Engineering — Building Technology — Fire Research — Chemical Engineering[2]

THE INSTITUTE FOR COMPUTER SCIENCES AND TECHNOLOGY conducts research and provides scientific and technical services to aid Federal agencies in the selection, acquisition, application, and use of computer technology to improve effectiveness and economy in Government operations in accordance with Public Law 89-306 (40 U.S.C. 759), relevant Executive Orders, and other directives; carries out this mission by managing the Federal Information Processing Standards Program, developing Federal ADP standards guidelines, and managing Federal participation in ADP voluntary standardization activities; provides scientific and technological advisory services and assistance to Federal agencies; and provides the technical foundation for computer-related policies of the Federal Government. The Institute consists of the following centers:

Programming Science and Technology — Computer Systems Engineering.

[1]Headquarters and Laboratories at Gaithersburg, MD, unless otherwise noted;
mailing address Washington, DC 20234.
[2]Some divisions within the center are located at Boulder, CO 80303.

Electrical Parameters in 60-Hz Biological Exposure Systems and Their Measurement: A Primer

M. Misakian

Electrosystems Division
Center for Electronics and Electrical Engineering
National Bureau of Standards
Washington, DC 20234

U.S. DEPARTMENT OF COMMERCE, Malcolm Baldrige, Secretary

NATIONAL BUREAU OF STANDARDS, Ernest Ambler, Director

Issued April 1984

TABLE OF CONTENTS

Page

TABLE OF CONTENTS (continued)

LIST OF FIGURES

LIST OF TABLES

Electrical Parameters in 60-Hz Biological Exposure
Systems and Their Measurement: A Primer

ABSTRACT

This report presents material which is intended to provide assistance
in the measurement of a number of electrical parameters that are of
importance during bioeffects research involving 60-Hz electric and
magnetic fields. The parameters that are considered are the electric
field strength E, the magnetic induction or flux density B, field
uniformity, harmonic content, phase relations between field
components, and corona. Descriptions of the fields and methods for
their laboratory generation are surveyed. The text is purposely
elementary with references provided to aid the interested reader in
obtaining a fuller understanding of many of the topics. It is shown
that using relatively simple instrumentation, it is possible to
characterize reasonably well the electric and magnetic fields used in
animal exposure studies.

Key words: biological effects; corona; electric field; ELF; magnetic
field; power frequency; 60-Hz; transmission lines.

1. INTRODUCTION

Because of the interest in recent years of possible biological effects of
electric and magnetic fields from ac high voltage transmission lines, many
laboratory studies have been conducted, or are under way, to determine what
effects can be associated with these fields [1-8]. This report identifies a
number of electrical parameters which must be controlled during such laboratory
studies and describes procedures for their measurement. The report is intended
to serve as a measurement primer for those planning biological experiments with
60-Hz electric and magnetic fields, perhaps for the first time. The electrical
parameters which are considered are the electric field strength, E, the
magnetic induction, B, field uniformity, harmonic content, phase relations
between field components, and corona. Methods for generating 60-Hz electric
and magnetic fields are also briefly described.

It is noted that the parameters cited are a small subset of a larger list of
physical parameters with which an investigator must be concerned. For example,
such things as temperature, humidity, light and dark cycles (and the timing of
exposure), noise, vibrations, and short circuit currents during drinking of
water may also be of importance. The reader is referred to the literature for a
discussion of these and other parameters [9-12]. This report, while tutorial in
nature, assumes that the reader is familiar with the subjects of electricity and
magnetism as presented in an introductory college physics course.

2. AC TRANSMISSION LINE FIELDS

The electric and magnetic field lines of a single conductor energized with 60-Hz
voltage and located above a ground plane are shown schematically at some instant
in figure 1. The magnetic induction or flux density B at a point can be
represented as a vector that oscillates in magnitude at a frequency of 60-Hz
along a line tangent to a circular magnetic field line. Similarly, the electric
field strength, E, can be represented as an oscillating vector tangent to an
electric field line. These fields are sometimes referred to as single-phase ac
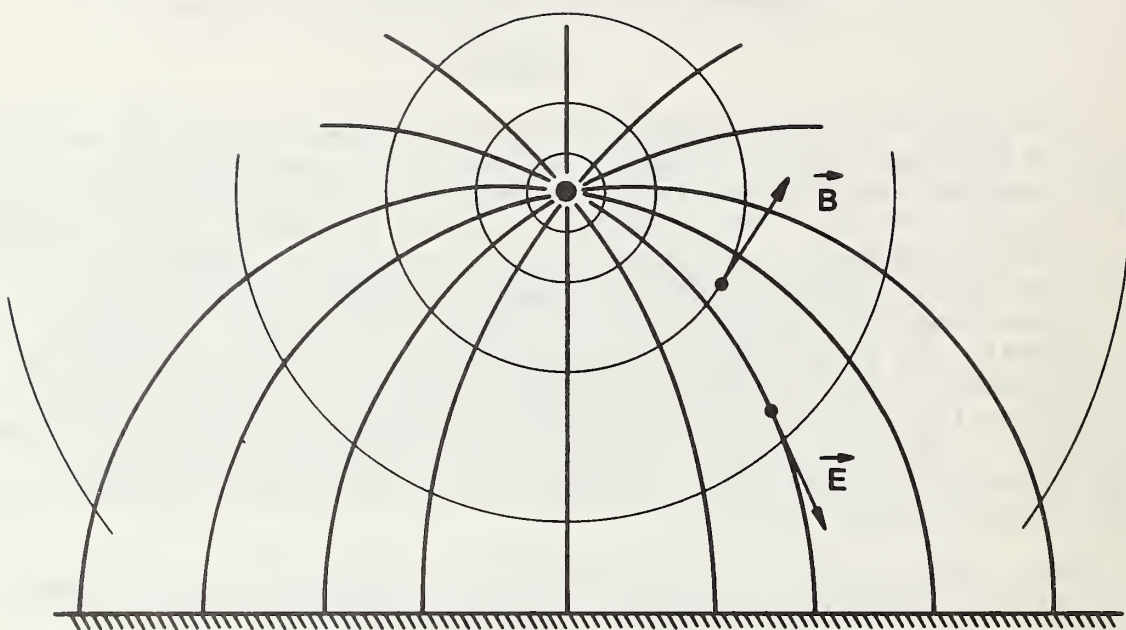fields [13].

Figure 1.   Electric and magnetic field lines of single conductor
above ground plane.
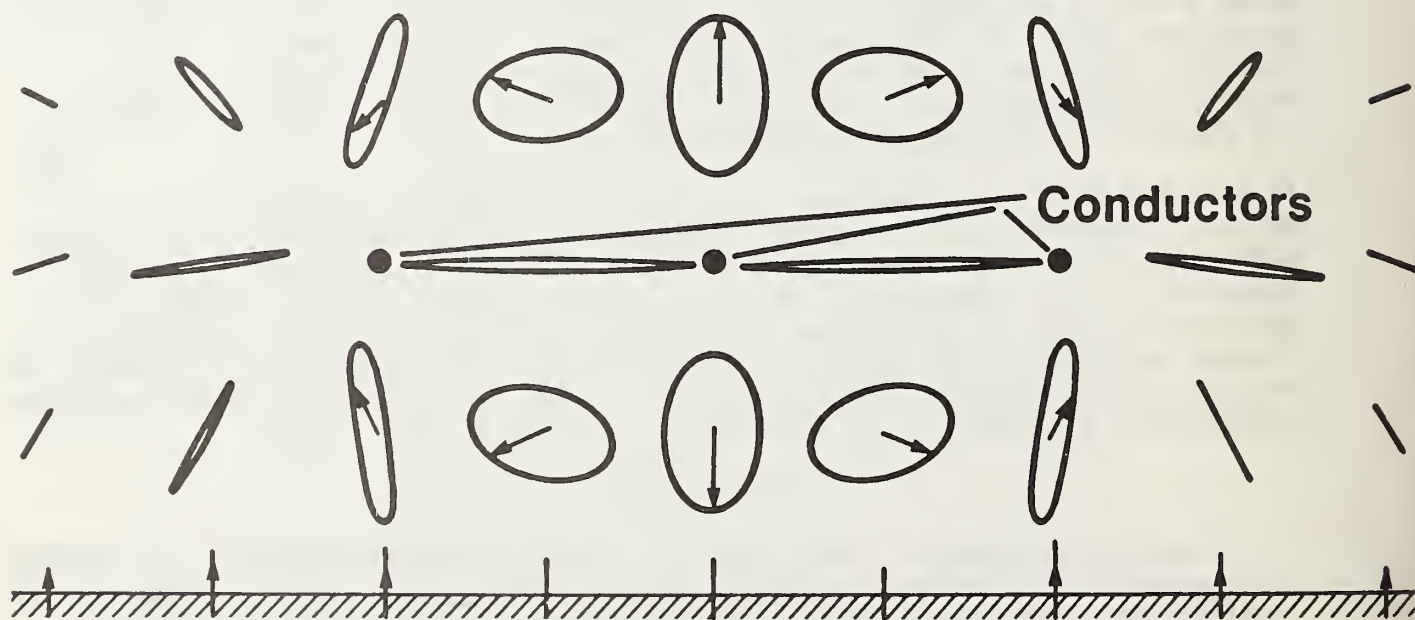
Figure 2.   Electric field ellipses in vicinity of 3-phase
transmission line.

2

Transmission lines normally have three or more conductors (or conductor bundles) with multiple voltage phases. The electric and magnetic fields of a three-phase transmission line have been calculated and illustrated by Deno [14] and a somewhat simplified sketch of the electric fields in the vicinity of a three-phase transmission line is given in figure 2. Three conductors are shown above the ground plane in figure 2 and the phase of the 60-Hz voltage applied to each conductor differs by 120° with respect to the conductor adjacent to it (e.g., sinusoidal voltages $V\sin(\omega t)$, $V\sin(\omega t + 120°)$, and $V\sin(\omega t + 240°)$ applied to adjacent conductors where V is the peak voltage).

In general, the electric field strength E at a point in space can be represented as a rotating vector which traces an ellipse in a plane perpendicular to the conductors as shown in figure 2. Near ground level, the field ellipse degenerates to a nearly vertical line. In the absence of nearby objects or irregular terrain, the field strength changes slowly from ground level to a height of about 1 or 2 meters, i.e., the field is approximately uniform. At ground level the field vector oscillates along a line perpendicular to the ground. Because of this spatial dependence of the transmission line electric field, laboratory simulations of the field at or near ground level can be made with a parallel plate apparatus (Section 3.1).

Although not shown in figure 2, the magnetic field at a point near a three-phase transmission line can also be represented by a rotating vector in space but in contrast to the electric field, the vector B is a rotating vector even at ground level [14]. Thus, laboratory simulation of a three-phase transmission line magnetic field near ground level requires an apparatus which can generate a rotating field (Section 3.6).

It can be shown that the elliptical representation of the fields for the three-phase, single-circuit transmission line shown in figure 2 is also relevant to lines with multiple circuits. That is, the fields from transmission lines, in general, can be represented by rotating vectors [15]. The maximum electric field strength near ground level within the right of way ranges in value from a few kV/m to about 9 kV/m, depending on the line voltage and conductor geometry. Similarly, the magnetic field can be as great as 0.3×10^{-4} tesla (0.3 gauss), depending on the current (load) and conductor geometry.

3. LABORATORY SIMULATION OF TRANSMISSION LINE FIELDS

As noted above, a parallel-plate apparatus can be used to generate the approximately uniform electric field that exists at or near the ground in the vicinity of a transmission line. Test animals have typically been placed in contact with the bottom plate and housed in plastic enclosures during exposure to the electric field [16].

Simulations of rotating transmission line magnetic fields can be obtained with two pairs of orthogonally oriented rectangular or square loops of many turns of wire or circular loops known as Helmholtz coils. Such systems can be used in conjunction with a parallel-plate, electric field apparatus to generate simultaneously 60-Hz electric and magnetic fields. The electric fields produced with parallel plates and the magnetic fields produced with orthogonally oriented coils of wire are described in further detail in the next two sections. While fields that are highly uniform can be generated with the systems that are described, ambient electric and magnetic fields with variations of about ±5% with respect to the fields at some central point have frequently been used in

experiments. What is considered acceptable field uniformity in a given experiment must be determined by the researchers.

It should be noted that throughout this report the sinusoidal time dependence of E and B and associated voltages and currents will be suppressed; use of root-mean-square (r.m.s.) values for these quantities will be assumed. It is recalled that the r.m.s. or "effective value" of a sinusoidal current is equal to the steady (dc) current that is required to develop the same amount of heat as the ac current passing through the same resistance in the same time. The r.m.s. current is equal to the peak sinusoidal current divided by $\sqrt{2}$. Similarly the r.m.s. voltage, electric field strength, etc. are equal to their peak values divided by $\sqrt{2}$.

3.1 Electric Fields Between Parallel Plates

Regions of nearly uniform electric field strength of known magnitude can be produced with a parallel plate system provided that the spacing of the plates, relative to the plate dimensions, is sufficiently small. The uniform field value E_0 is given by V/t where V is the applied potential difference between the plates and t is the plate spacing. The magnitudes of the normalized field, E/E_0, at the plate surfaces and in the midplane of semi-infinite parallel plates can be theoretically determined [17] and are plotted as a function of normalized distance x/t from the plate edge in figure 3; numerical values are given in Table 1.

The numerical values in Table 1 show that the departure from field uniformity due to fringing field effects is 0.1% at a distance of one plate spacing from the edge. For finite square plates, the fringing field effects from four edges can be estimated by superposition when the effect from one edge is less than 0.2%. For example, when the side dimension of a square parallel plate system is twice the plate spacing, the field strength at the center of the plate surfaces is approximately 0.4% greater than E_0. These results are valid in the absence of perturbations due to nearby grounded objects such as walls, floors, equipment, etc. (The perturbations due to non-grounded objects is, in general, less.)

A numerical calculation of the electric field between finite square parallel plates has been reported in the literature [18]. Profiles of the electric field between the plates are provided for different ratios of plate dimension to plate spacing. This calculation also assumes the absence of perturbations due to nearby ground planes.

3.1.1 Stray Electric Fields and Shielding

While attention in Section 3.1 focuses on the field between the parallel plates, it should be remembered that the electric field also extends to regions beyond the plates [17]. Thus, if sham exposed (control) animals are located nearby, electrical shielding may be necessary for these animals. Use of grounded metal screen or hardware cloth readily reduces the field strength to ambient levels.

3.2 Energizing Parallel Plates

The parallel plates can be energized with a commercially available high voltage power supply or with a variable autotransformer-transformer combination. A voltage regulator or line conditioner is frequently used to prevent fluctuations of the line voltage to the autotransformer. An oscillator and power amplifier
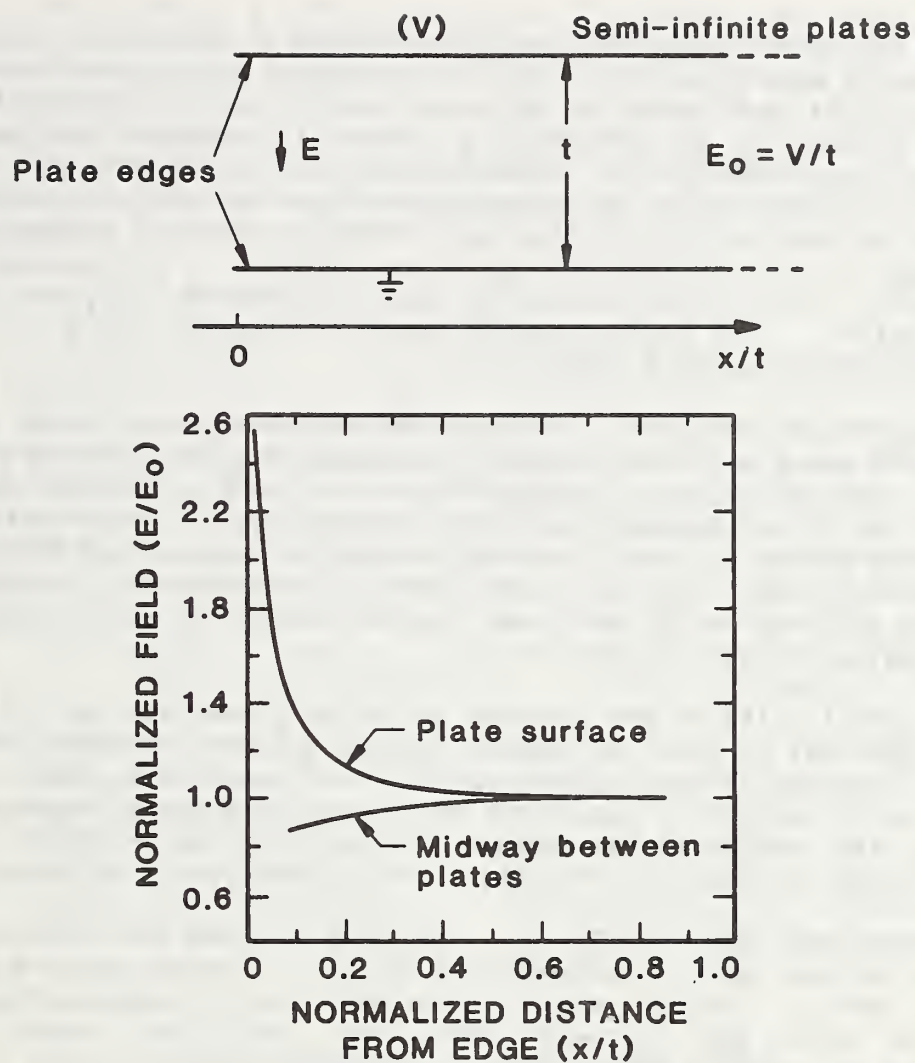
Figure 3.   Normalized electric field at the surfaces of and midway between semi-infinite parallel plates.

Table 1.   Normalized electric field strength midway between plates and at plate surfaces

Midway Between Plates			Plate Surface	
x/t	E/E_0		x/t	E/E_0
0.0698	0.837		0.0185	2.449
0.1621	0.894		0.0829	1.414
0.2965	0.949		0.1230	1.265
0.4177	0.975		0.1624	1.183
0.6821	0.995		0.2431	1.095
0.7934	0.997		0.4376	1.025
1.0000	0.999		0.6861	1.005
			0.7954	1.002
			1.0000	1.001

can also be used in place of the autotransformer. Systems for energizing the plates should have provisions made for continuous metering of the voltage to the plates, e.g., a panel meter on the power supply (during "double-blind" field exposure studies, it may be necessary to make arrangements for recording the "field-on" condition without visual cues for the investigators). While the voltage across the plates can be measured with a calibrated electrostatic voltmeter or high voltage divider and correlated with the voltage setting on the power supply, it is perhaps more useful to establish a correspondence between the electric field, which is readily measured (Section 4.1), and the power supply setting. This correspondence should be checked regularly to insure repeatable field exposure conditions.

Center-tap transformers which produce two high voltages of equal magnitude but of opposite phase and "single-ended" transformers which produce a single high voltage relative to ground potential have been used to energize the parallel plates. The former approach minimizes perturbations of the electric field between the plates by nearby grounded objects or planes (see below). With certain precautions taken to minimize corona (see Section 5), electric field strengths as large as 100 kV/m have been produced with parallel plate systems for biological studies [19].

Because lethal voltages and currents are usually generated by the power supply, precautions must be taken to prevent contact between personnel and the high voltage leads and parallel plates during field exposure periods. The parallel plates can be located in rooms with door interlocks which, when opened, interrupt the voltage to the plates. Current limiting resistors in the high voltage leads to the parallel plates can also be used as an added precaution.

Isolation of the power supply in a room separate from the parallel plates may be required in some cases to prevent audible noise from the power supply reaching the test animals. Vibrations of the parallel plates because of sinusoidal electrical forces may also be of concern [9]. Additional remarks regarding the energizing of parallel plates during experiments employing both electric and magnetic fields are given in Section 3.6.

3.3 Perturbations of Electric Field

Two types of field perturbations are distinguished in this report. The first, over which control is not normally attempted, is the perturbation of the field near and at the surface of a test animal. This perturbation depends on the animal's geometry and electric potential. The second type of field perturbation, over which some control can and should be exercised, is produced by factors that influence the ambient field strength (i.e., as shown in fig. 3) prior to the introduction of the test animal between the parallel plates or influence the "normal" geometric field perturbation at or near the surface of the test animal after it is placed into the field. Field perturbations of the second type are considered next.

3.3.1 Parallel Plate Spacing

While the information in Table 1 is useful for estimating the dimensions of a parallel plate system which has extended regions of field uniformity, the size of the test animal can influence the choice of spacing between the plates. The parallel plate spacing should be sufficiently large in order to avoid significant perturbation of the surface charge distribution on the top plate by the presence of the animal [19]. The measurements of Kaune [20] indicate that a

6

model animal in the shape of a hemi-ellipsoid on the bottom plate does not significantly interact with the top plate charge distribution when the height of the hemi-ellipsoid is as much as 28% of the plate spacing. Failure to provide adequate spacing between the plates leads to a field-induced current in the animal that is larger than that produced by an ambient field of the same magnitude but with greater parallel plate spacing. Alternatively, it can be said that inadequate plate spacing can increase the field strength at the surface of the animal beyond that caused solely by the animal's shape.

3.3.2 Perturbations by Nearby Ground Planes

The electric field values shown in figure 3 and Table 1 have been determined assuming that there are no objects or ground planes nearby. In the presence of ground planes, which can be approximated by a wall, floor, or ceiling, the surface charge distributions on the parallel plates are perturbed and lead to changes in the electric field. If one of the plates is grounded, the perturbations can be quite large, particularly near the plate edge [21,22]. For example, measurements have shown that the surface field strength near the edge of a grounded plate can be reduced by more than 10% when a vertical ground plane is two plate-spacings away from the edge of the parallel plates [21]. In general, the field strength is reduced at the grounded plate and increased at the energized plate; corresponding changes occur at points between the plates.

Since the unperturbed field on the plate surfaces increases as the edges are approached (fig. 3), some reduction in field strength near the edge of the grounded plate may be desirable in order to obtain a greater region of approximately uniform field where the test animals are located. The perturbations due to nearby ground planes can be reduced by using a center-tap transformer to energize the parallel plates. In any event, the variation of the field strength where test animals will be placed for exposure should be characterized and this is readily accomplished with the instrumentation described in Section 4.1.

3.3.3 Perturbations by Objects Between Plates

Introduction of objects with large dielectric constants such as food or a plastic bottle filled with water between the parallel plates can cause significant perturbations of the field. Figure 4 shows a schematic view of a plastic animal enclosure containing food and water, and which has been used for exposing animals to 60-Hz electric fields. The water and metal mesh floor are electrically connected to reduce the possibility of spark discharges between the animal and water when the animal drinks. The field strength values with and without parentheses in figure 4 represent measurements performed with the enclosure removed and present, respectively. The measurements in the enclosure reveal a low field region below the bottle that is approximately a third of the uniform field value between the plates [23].

The influence of plastic enclosures on the field distribution at the surface of a test animal has been studied by Kaune [20]. By measuring induced currents on isolated conductive patches on a hemi-ellipsoid animal model, he has demonstrated that the surface fields can be increased or decreased depending on the position of the animal relative to the plastic enclosure and the location on the surface of the animal. Contamination of the plastic surface from animal contacts can also have significant effects on the field. Decreases in field strength of 49% within an enclosure have been observed after rats have occupied the enclosure for 16 days [24].
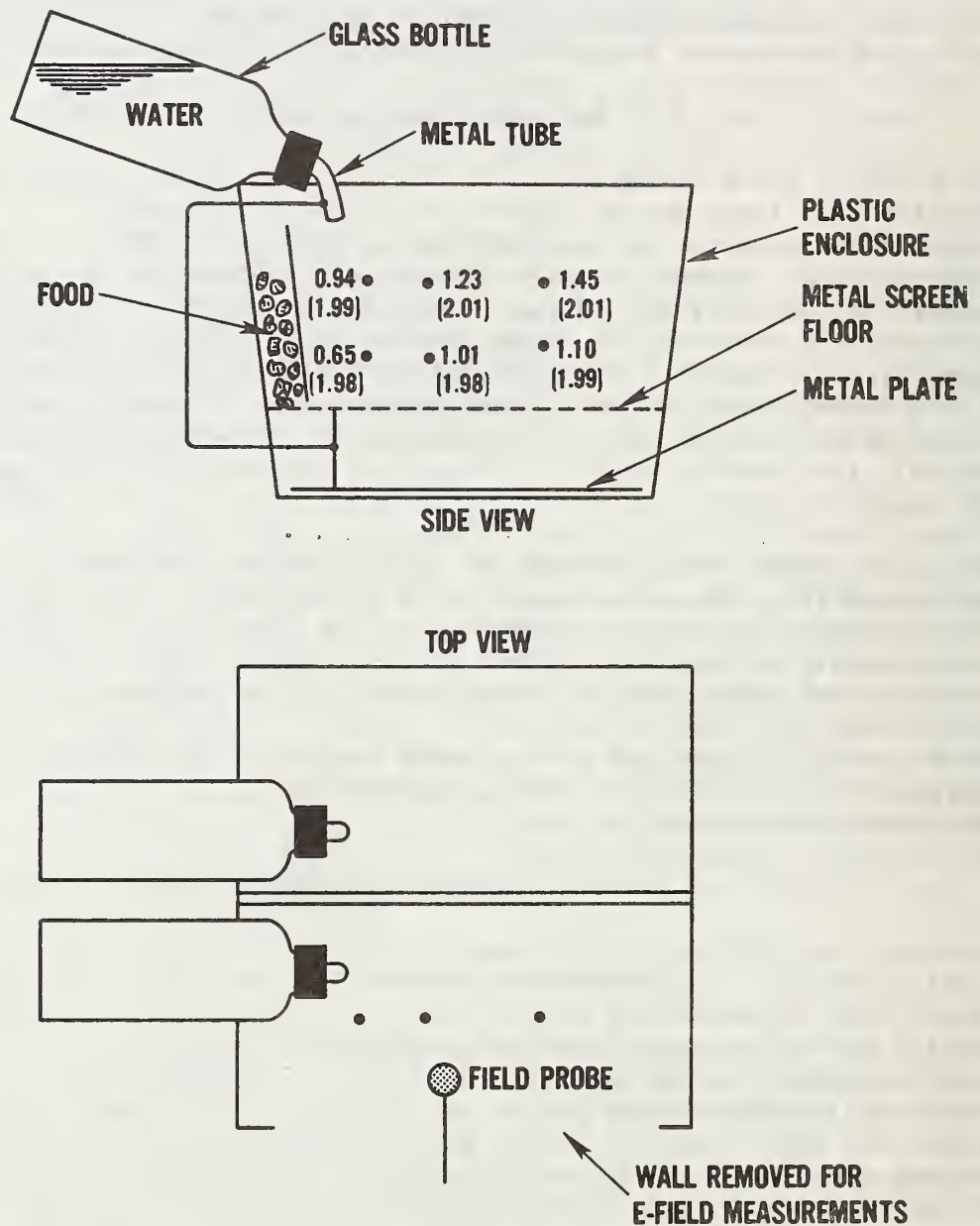
Figure 4. Perturbations of electric field in plastic enclosure due to presence of water bottle, food, and plastic. The relative field strength values prior to the introduction of the enclosure and water bottle are shown in parenthesis.

3.3.4 Mutual Shielding of Test Animals

The last source of field perturbation which is considered is caused by the placement of more than one animal into the exposure system. While actually another example of the type of perturbation considered in 3.3.3, it is treated separately here to emphasize its importance.

Some animals, such as mice, if placed into the same plastic enclosure may "pile up" and thereby change the field distribution at the surface of each animal. By separating the animals with a partitioned plastic enclosure, the interactions between the animals is reduced. However, the mutual shielding caused by the proximity of adjacent rats, as determined by measurement of the total induced (or short-circuit) current in an animal, has been found to be as large as about 35% under certain conditions [20]. Model animals in the shape of hemi-ellipsoids with conductive coatings can be placed adjacent to animals that are along the perimeter of a partitioned enclosure to provide comparable field exposure conditions for all the animals [25].

3.4 Magnetic Field of Rectangular Loops of Many Turns

Figure 5 shows two rectangular loops of many turns of wire of dimensions 2a x 2b separated by a distance s. The z-component of the magnetic flux density at a point P(x,y,z) due to a current in the lower loop is given by the expression [21].

$$ B_{z1} = \frac{\mu_0}{4\pi} \, IN \sum_{\alpha=1}^{4} \left[\frac{(-1)^\alpha d_\alpha}{r_\alpha [r_\alpha + (-1)^{\alpha+1} C_\alpha]} - \frac{C_\alpha}{r_\alpha (r_\alpha + d_\alpha)} \right] \tag{1} $$

where

$$ C_1 = -C_4 = a+x \qquad\qquad r_1 = \sqrt{(a+x)^2 + (b+y)^2 + z^2} $$

$$ C_2 = -C_3 = a-x \qquad\qquad r_2 = \sqrt{(a-x)^2 + (b+y)^2 + z^2} $$

$$ d_1 = d_2 = y+b \qquad\qquad r_3 = \sqrt{(a-x)^2 + (b-y)^2 + z^2} $$

$$ d_3 = d_4 = y-b \qquad\qquad r_4 = \sqrt{(a+x)^2 + (b-y)^2 + z^2} $$

N is the number of turns, I is the current and μ_0 is the magnetic permeabilit, of air. The conductors in the loop are assumed to be of negligible cross section. By superposition of fields, the flux density at P(x,y,z) due to a current I in both loops assuming the same number of turns in each loop, is

$$ B_z = B_{z1} + \frac{\mu_0}{4\pi} \, IN \sum_{\alpha=1}^{4} \left[\frac{(-1)^\alpha d_\alpha}{r'_\alpha [r'_\alpha + (-1)^{\alpha+1} C_\alpha]} - \frac{C_\alpha}{r'_\alpha (r'_\alpha + d_\alpha)} \right] \tag{2} $$
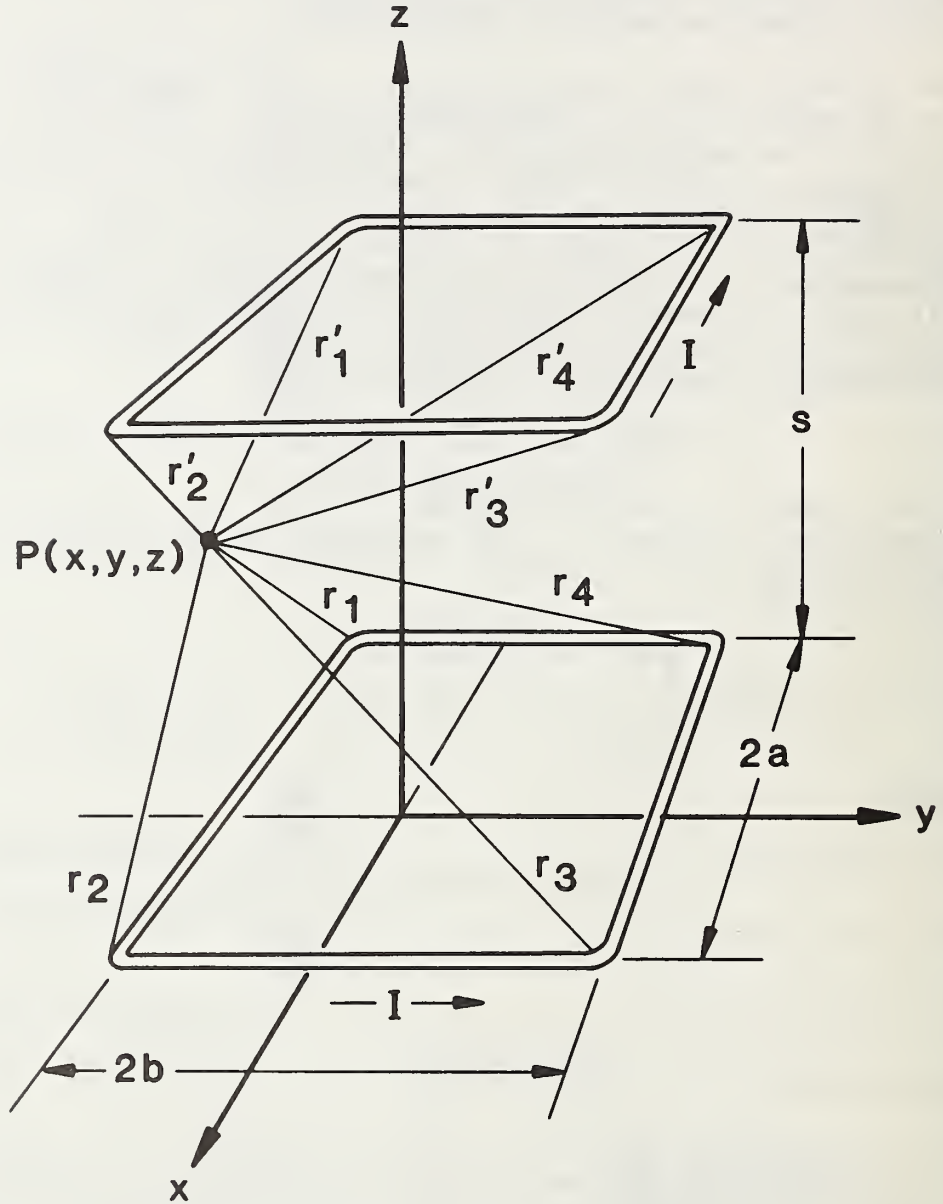
where

Figure 5. Coordinate system and configuration of rectangular loops for generating magnetic field.

$$r_1' = \sqrt{(a+x)^2 + (b+y)^2 + (s-z)^2}$$

$$r_2' = \sqrt{(a-x)^2 + (b+y)^2 + (s-z)^2}$$

$$r_3' = \sqrt{(a-x)^2 + (b-y)^2 + (s-z)^2}$$

$$r_4' = \sqrt{(a+x)^2 + (b-y)^2 + (s-z)^2}$$

It can also be shown that the x and y-components of the flux density for the two loops are given by [26]

$$B_x = \frac{\mu_o}{4\pi} IN \sum_{\alpha=1}^{4} \left[\frac{(-1)^{\alpha+1} z}{r_\alpha(r_\alpha + d_\alpha)} + \frac{(-1)^{\alpha}(s-z)}{r_\alpha'(r_\alpha' + d_\alpha)} \right] \qquad (3)$$

$$B_y = \frac{\mu_o}{4\pi} IN \sum_{\alpha=1}^{4} \left[\frac{(-1)^{\alpha+1} z}{r_\alpha [r_\alpha + (-1)^{\alpha+1} C]} + \frac{(-1)^{\alpha}(s-z)}{r_\alpha' [r_\alpha' + (-1)^{\alpha+1} C]} \right] \qquad (4)$$

Figure 6 shows the variation along the z-axis of the normalized flux density, $B/B(0,0,0.25)$, for square coils of 1 m side dimension and 0.5 m spacing (because of symmetry considerations, B_x and B_y vanish along the z-axis and B_z is equal to the total flux density B). Also shown are the variations of the normalized x, y, and z-components of the flux density along a vertical line passing through the point (0.25, 0.25, 0). The corresponding numerical values are given in Table 2. It is evident that for this sample calculation, the flux density is within 4% of B(0, 0, 0.25) in a central volume of 20 cm x 20 cm x 20 cm.

Beginning with eq. (1), the principle of superposition can be used to develop expressions for the magnetic induction due to two or more rectangular loops of many turns with different values of a, b, N and spacing provided that their z-axes coincide.

It should be noted that the magnitude and time dependence of the magnetic flux density at a point is determined by the sinusoidal current I once the dimensions, a and b, and the number of turns, N, of the field windings have been fixed.

3.5 Helmholtz Coil Magnetic Field

The z-component of the magnetic flux density at a point $P(r,\theta)$, between two coils of radius b with N turns of wire separated by a distance of 2d as shown in figure 7 is given by [27]

$$B_z(r,\theta) = \frac{\mu_o Ib^2 N}{2(b^2+d^2)^{1.5}} [2+A_2 P_2(\cos\theta)r^2 + A_4 P_4(\cos\theta)r^4 + \ldots] \qquad (5)$$

where

$$A_2 = \frac{15d^2 - 3(b^2+d^2)}{(b^2+d^2)^2}$$

$$A_4 = \frac{15(b^2+d^2)^2 - 210d^2(b^2+d^2) + 315d^4}{4(b^2+d^2)^4}$$

11

NORMALIZED FLUX DENSITY

1.2 — $B_z(0.25,0.25,z)/B(0,0,0.25)$

1.0

$B_z(0,0,z)/B(0,0,0.25)$

0.8

|← 20 cm →|

0.02

0

$B_x(0.25,0.25,z)/B(0,0,0.25)$

-0.02 — $B_y(0.25,0.25,z)/B(0,0,0.25)$

0   10   20   30   40   50

HEIGHT ABOVE BOTTOM COIL (z,cm)
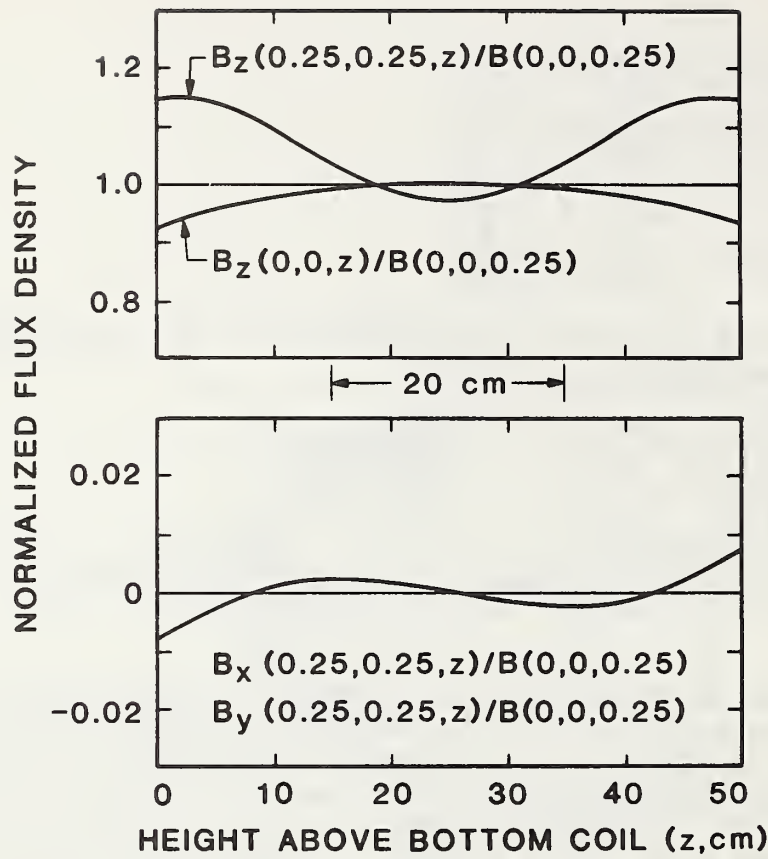
Figure 6.   Normalized flux density profiles along z-axis and along
vertical line through point x = 0.25 m, y = 0.25 m. The
magnetic field is produced with two square coils of 1 m
side dimension and separated by a distance of 0.5 m.

Table 2. Normalized flux density profiles

z(cm)	$B_z(0,0,z)/B(0,0,0.25)$	$B_z(0.25,0.25,z)/B(0,0,0.25)$	$B_{x,y}^{*}(0.25,0.25,z)/B(0,0,0.25)$
0	0.9335	1.1476	-0.0807
5	0.9637	1.1471	-0.0247
10	0.9830	1.0994	0.0128
15	0.9937	1.0377	0.0254
20	0.9986	0.9903	0.0179
25	1.0000	0.9730	0.0000
30	0.9986	0.9903	-0.0179
35	0.9937	1.0377	-0.0254
40	0.9830	1.0994	-0.0128
45	0.9637	1.1471	0.0247
50	0.9335	1.1476	0.0807

*Negative sign indicates reversal of field direction.
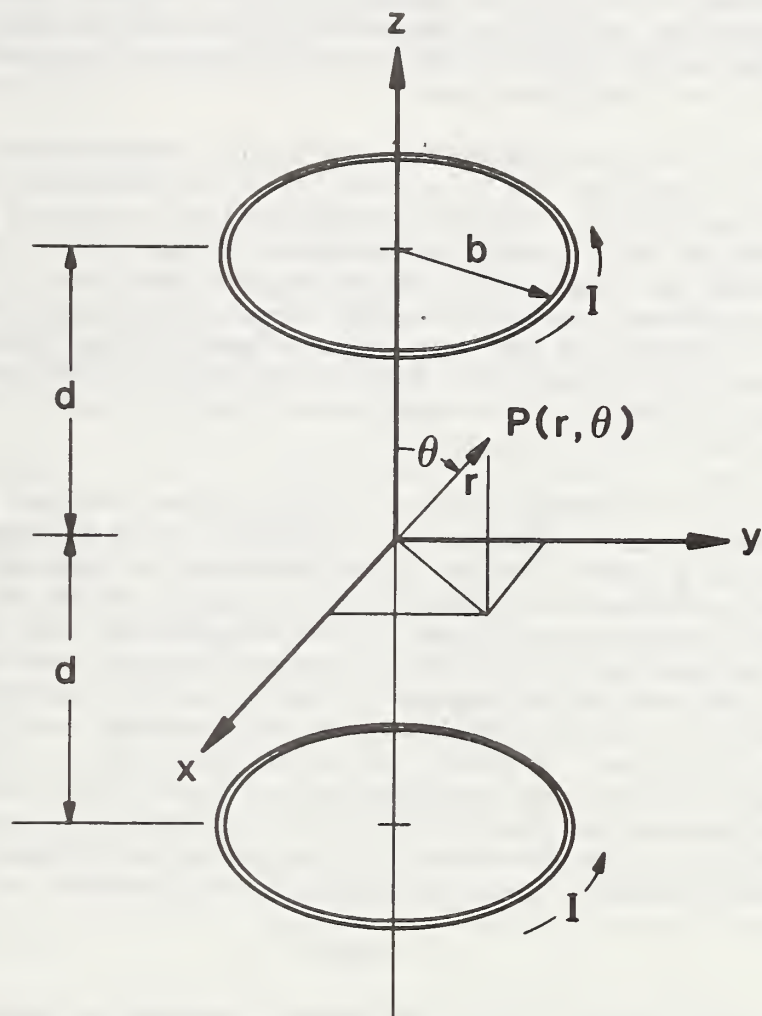
Figure 7. Configuration of coils for generating magnetic field and coordinate system.

μ_0 is the permeability, I is the current, r and θ are spherical coordinates, and $P_m(\cos\theta)$ are Legendre polynomials of order m; the conductor cross sections are again assumed to be negligible.

For the condition 2d = b, A_2 vanishes and the field becomes highly uniform in a small volume near the origin. For example, in a region $|z-(b/2)|<(b/10)$ along the z-axis (i.e., θ = 0), $B_z(z)$ varies from the central value by less than 0.012%. Coils that satisfy the condition 2d = b are known as Helmholtz coils. The horizontal field component can be calculated but only with some difficulty [28,29] and is not considered here.

3.5.1 Stray Magnetic Fields and Shielding

Equations (2) to (5) show that the magnetic field decreases as a function of distance from the field generating loops and coils. For example, the magnetic induction along the z-axis for a set of square loops 1 m x 1 m and 0.5 m spacing decreases to 0.44% of the central value (between the loops) at a distance of 3.75 m from the center of the loop. For a central flux density of 2×10^{-4} tesla (2 gauss), the stray field 3.75 m away is 8.8×10^{-7} tesla (8.8 milligauss) which is more than three times the ambient magnetic field levels reportedly found in homes [30].

Preventing stray ac magnetic fields produced by an exposure system from reaching a sham exposed group of animals is, in general, more difficult and costly than shielding 60-Hz electric fields. Metal sheets with large permeability or high conductivity can be used for attenuating the stray fields to an "acceptable" (to be set by the investigators) level if the exposed and sham exposed animals cannot be separated with sufficient distance. Metals with large permeabilities concentrate and confine the magnetic field lines to a degree that depends on the angle of incidence of the flux lines and the permeability [31]. Limited attenuation also occurs in metals of low permeability, but good conductivity, such as copper because the varying magnetic field induces eddy currents in the metal which reduces the flux density. The distance into the metal at which the magnetic field is attenuated to e^{-1} of its value at the metal surface is known as the skin depth and is given for copper by the expression [32]

$$\delta = 0.066/f^{0.5} \qquad (6)$$

where f is the frequency of the field and δ is given in meters. For 60-Hz magnetic fields, the skin depth is nearly 1 cm. If shielding is required, a trial and error approach using metal sheets of high permeability and good conductivity followed by measurements of the residual field may be the most expeditious way to develop adequate shielding for the sham exposed animals.

3.6 Energizing Magnetic Field Coils

Current to the magnetic field coils can be provided with a variable auto-transformer and current limiting resistor. As in the case of energizing the parallel plates, use of a voltage regulator or line conditioner is desirable to reduce fluctuations of the line voltage to the autotransformer. Also, as before, an oscillator-power amplifier combination may be used in the place of the variable autotransformer. Knowledge of the current limiting resistance and measurement of the voltage across the resistor allows one to determine the current, I, using Ohm's law. The flux density can then be calculated from

equations (2) to (5). It is assumed here that the power rating of the current limiting resistor is large enough to prevent significant change in resistance value due to heating.

As noted in Section 2, the magnetic field from a three-phase transmission line is a rotating magnetic field in a vertical plane at and near ground level. Circularly polarized magnetic fields rotating in a vertical plane have recently been adopted for use in the animal field exposure studies sponsored by the State of New York Department of Health [8] and the production of such fields is briefly considered here.

Circularly polarized magnetic fields can be produced at a point by two sets of orthogonally oriented magnetic field loops or coils provided that the field components there are equal in magnitude and differ in phase by 90°. If the magnetic field components can be made nearly uniform in an exposure system where test animals will be located, the animals will experience an approximately circularly polarized magnetic field. Because the time dependence of the field components is a function of the sinusoidal currents to the coils, the 90° phase difference between the field components is obtained by phase-shifting the current to one of the coils by 90° with respect to the other coil.

Figure 8 is a schematic view of an apparatus which permits simultaneous excitation of two sets of orthogonally oriented magnetic field coils and a parallel plate electric field apparatus. If the impedance in the circuits to the vertical field coil is dominated by the current limiting resistor and wire resistance (and not the inductance of the coils), the vertical component of the magnetic field and the electric field will be nearly in phase because the current to the coil and the voltage applied to the plates will be in near phase coincidence. The phase of the horizontal magnetic field component can be made to differ from the vertical magnetic field by 90° by using the phase shifter.

The phase relationships between the electric and magnetic fields described above are being used in the New York State-sponsored small animal studies. While fixing the phase relationships between the fields is considered arbitrary at this time because of the state of knowledge of power frequency field effects, the practice insures a degree of consistency in exposure conditions for the various investigations.

The schematic view of an exposure system in figure 8 is shown for illustrative purposes and is not intended as a recommended design for an exposure apparatus. Other arrangements such as employing more than two loops or coils along a given axis (with unequal turns) or energizing the coils and plates with three-phase line voltage can be used [33].

A final engineering note is that the current carrying capacity of insulated wire used in the magnetic field windings may have to be reduced from the value specified by the manufacturer in air because of excessive heating effects that can occur in the "bundled" configuration.

3.7 Perturbations of Magnetic Field

The number of mechanisms for perturbing the magnetic field are fewer than for the electric field case. Ferromagnetic materials such as iron and nickel can
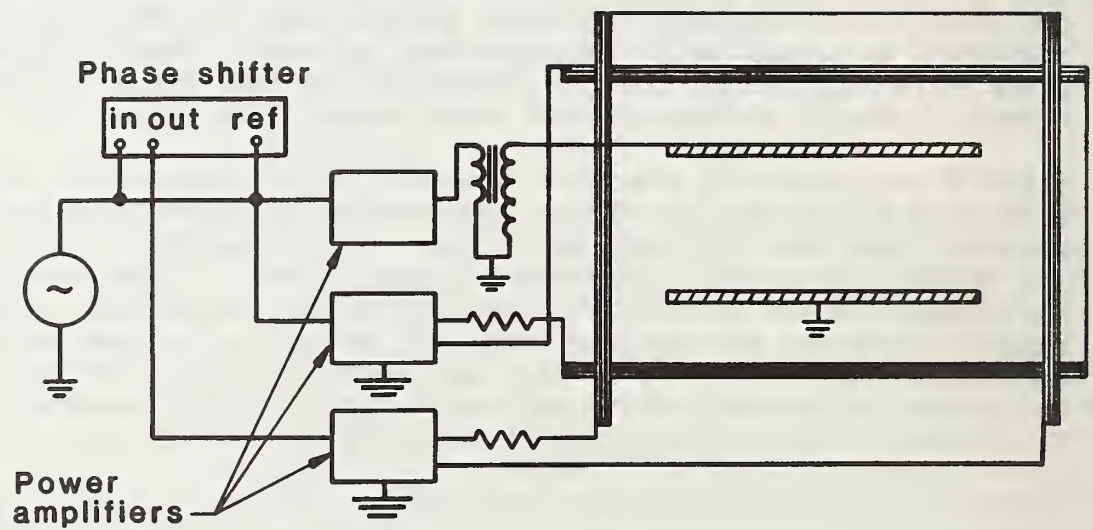
Figure 8. Schematic view of apparatus for simultaneously
generating an electric field and a rotating magnetic
field.

cause large perturbations when introduced into a magnetic field but their use is readily avoided in field exposure studies. Most other (non-ferromagnetic) materials exhibit the weaker magnetic effects of paramagnetism and diamagnetism [34] and perturb the field to a degree that can normally be neglected. Non-ferromagnetic conductors such as copper and aluminum are "exceptions to the rule" because the ambient magnetic field varies with time and induces eddy currents which can lead to perturbation of the magnitude and phase of the magnetic field. The magnitude of the perturbation increases with eddy current and decreases with distance from the conductor. Because parallel plate conductors are used to generate the electric field in exposure systems that employ electric and magnetic fields simultaneously, and test animals are usually located on the surface of the bottom plate, the eddy current perturbations must be characterized (measured) and, if necessary, reduced to an acceptable level. Perhaps the most direct approach for reducing the perturbation is to reduce the eddy currents by decreasing the conductivity of the parallel plate electrodes. Techniques that have been employed include using thin metal foil mounted on dielectric surfaces for the plates, partitioning the plate into smaller but connected sections, and using wide mesh metal screen for the bottom plate. Methods for characterizing the perturbation of the magnetic field are discussed in Section 4.5.

4. MEASUREMENT OF FIELD PARAMETERS

4.1 Electric Field Measurements

The measurement instrumentation which is considered here is intended for use in exposure systems that are typically employed for small animal studies. The electric fields in larger exposure systems, such as might be used for human experiments, may be characterized with commercially available electric field strength meters that are used for measurments in the vicinity of transmission lines [13]. These probes are, in general, too large for use between parallel plates employed for small animal studies (with spacings of the order of 0.5 m) because of excessive interaction between the fieldmeter and the surface charge distributions on the parallel plates.

Electric field strength measurements at the surface of a grounded bottom plate of a parallel plate system are readily performed with the simple instrumentation shown schematically in figure 9. A circular or square electrode fabricated from double copper-clad printed circuit board serves as the sensing probe, and a current-to-voltage operational amplifier circuit and digital voltmeter act as the detector of an electric field strength meter [35]. The fieldmeter shown in figure 9 determines the field strength, averaged over the area of the sensing electrode, by measuring the current induced into the sensing electrode. Using Gauss' law, it is readily shown that the relation between the electric field strength at the surface of the electrode, E, and the induced current, I, is

$$I = 2\pi f \epsilon_0 AE \qquad (6)$$

where f is the frequency of the sinusoidal field, ϵ_0 is the permittivity of free space and A is the area of the sensing electrode. For example, the current induced in a probe with a sensing area of 100 cm^2 placed in a 10 kV/m electric field is about 0.33×10^{-6} amperes (due to the finite thickness of the probe and
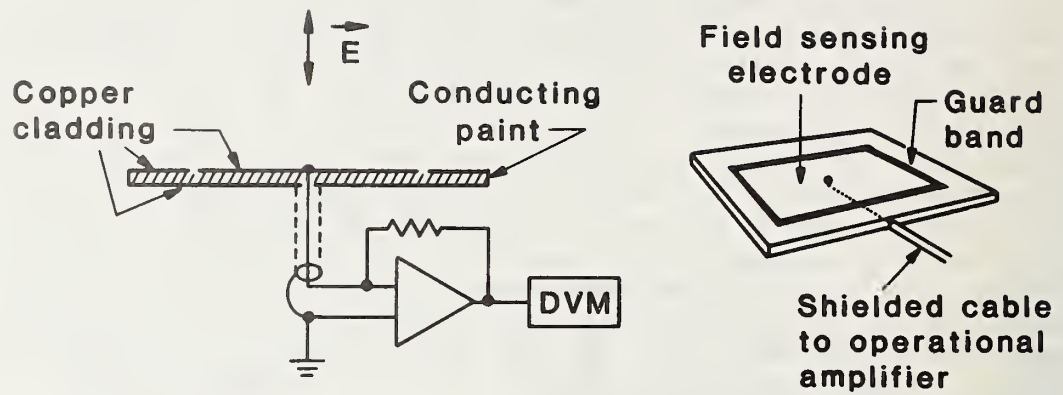
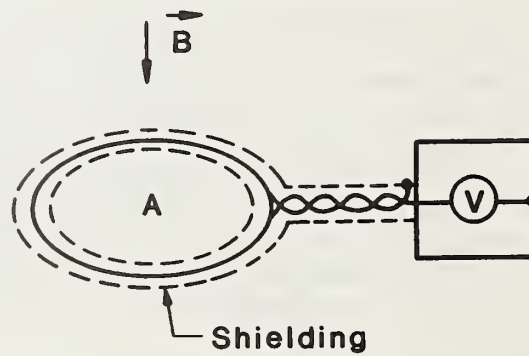Figure 9. Schematic view of flat probe-type electric fieldmeter.

Figure 10. Schematic view of coil-type magnetic fieldmeter.

the resultant field enhancement, the current is slightly higher). The output voltage of the operational amplifier circuit (fig. 9) with a 1 megohm feedback resistor would therefore be 0.33 volts. The detector circuit is shielded to avoid electrical pick-up, and is usually located outside the parallel plate system for remote observations. Microminiature coaxial cable with aluminized plastic shielding is commercially available and is very effective in reducing electrical pick-up. The calibration of the fieldmeter is performed with a parallel plate system and is discussed further in Section 4.3.1. A fieldmeter similar to that shown in figure 9 has been used for mapping electric field profiles on the bottom plates of parallel plate exposure systems [22].

If the parallel plates are energized with a center-tapped transformer, the fieldmeter described above can still be used for field strength measurements provided that the detector (i.e., operational amplifier circuit and digital voltmeter) is no longer referenced to ground but to the potential of the bottom plate. For large parallel plates, this is readily accomplished by using a battery-operated detector housed in a metal box and placed on the bottom plate. A small screened window permits viewing of the digital voltmeter display from a distance. The perturbing influence of the box on the field measurement can be checked by introducing a second identical box at a location equal in distance from the probe as the detector and observing the difference in field strength value. Tests have shown that a detector housed in a metal box with dimensions (length x width x height) of 21 cm x 16 cm x 7 cm does not measurably affect the electric field near a disk probe, 10 cm in diameter, located 50 cm away. The parallel plate spacing was 50 cm during these tests. Flat, electrically floating, probes have been successfully used to characterize the electric field strength at the surface of energized plates in biological exposure systems [36].

Electric field strength measurements at points between the parallel plates can be made with several types of fieldmeters, but the complexity and cost of the instrumentation is much greater than devices described above. Miniaturized free-body type probes connected to a portion of the detector with a fiber-optic link have been developed in recent years [37]. Fieldmeters which utilize the Pockel's effect have also been developed [38]. A miniature fieldmeter with wire connections between the probe and detector [39] is described in the Appendix.

4.2 Magnetic Field Measurements

Power frequency magnetic fields can be measured with a fieldmeter consisting of an electrically shielded coil of wire (probe) and a portable voltmeter detector shown schematically in figure 10. The principle of operation of the fieldmeter makes use of Faraday's Law which predicts that an electromotive force (emf) is produced at the ends of an open loop of wire placed in a changing magnetic field. For a loop of N turns placed in a sinusoidally varying field with frequency f, the emf is

$$emf = 2\pi fNAB \qquad (7)$$

where B is the flux density perpendicular to the area, A, of the loop. It is assumed that the magnetic field due to the induced current in the probe (after the probe is connected to a voltmeter) is small enough to be ignored. The emf produced by a coil of 500 turns and an area of 100 cm^2 when placed in a field of 10^{-4} tesla (1 gauss) is 0.189 volts. The coil probe and voltmeter detector

should be well shielded to prevent electrical pick-up, particularly when electric fields from an exposure system are present. Calibration of magnetic fieldmeters is discussed in Section 4.3.2.

Coil-type magnetic fieldmeters can be readily fabricated and are also commercially available. Hall effect magnetic fieldmeters which are commercially available can also be used for 60-Hz magnetic field measurements. However, such fieldmeters tend to have insufficient sensitivity for measurement near ambient (10^{-7} tesla) flux densities.

4.3 Fieldmeter Calibration

The systems described earlier in Section 3 for generating electric and magnetic fields can also be used for calibation purposes. Examples of calibration apparatus for electric and magnetic fieldmeters are presented below.

4.3.1 Electric Fieldmeters

Calibration of the flat electric field probes described in Section 4.1 is readily accomplished using a parallel plate system with a grounded bottom plate. The probe is placed on the bottom plate which has dimensions sufficiently large so that the edges of probe are no closer than two plate spacings to any edge of the bottom plate. The spacing between the plates should be at least as large as one and one-half times the side dimension of the probe, for probes with thicknesses of 3 percent or less of the (probe) side dimension, to insure that there is no significant perturbation of the surface charge distributions on the top plate due to the presence of the probe. The guard band should be at least as wide as 6% of the side dimension of the probe. Nearby ground planes (e.g., floor, walls) should be no closer than two plate spacings away from the parallel plates. With the above restrictions, the calibration electric field will be within 0.5% of the uniform field value, V/t (uncertainties in the value of V and t will add to the 0.5%).

Procedures for calibration of electric fieldmeters which can measure the field strength at points above the bottom plate are described elsewhere [13, 40] and are not discussed here.

4.3.2 Magnetic Fieldmeters

Calibration of a magnetic fieldmeter is typically performed by introducing the probe into a nearly uniform magnetic field of known magnitude and direction. Helmholtz coils (Section 3.5) have frequently been employed to generate such fields but the more simply constructed single loop of many turns with rectangular geometry can also be used. The simplicity in construction is at the expense of reduced uniformity, but sufficient accuracy is readily obtained. The z-component of the magnetic flux density is given by Eq. (1). It is noted for purposes of reference that $B_z(0,0,0) = \mu_0 IN\sqrt{2}/\pi a$ for a square loop of side dimension 2a. Equation 1 has been used to calculate the field values at and near the center of a square loop of dimensions 1 m x 1 m. Figure 11 shows percentage departure from the central magnetic field value at nearby points in the plane of the loop and 3 cm above and below the plane of the loop (indicated in parenthesis). Also shown in figure 11 is an approximate outline (scale drawing) of a commercially available magnetic field probe. A 1% change in the loop dimension changes the values over the probe by about 1%. For the probe
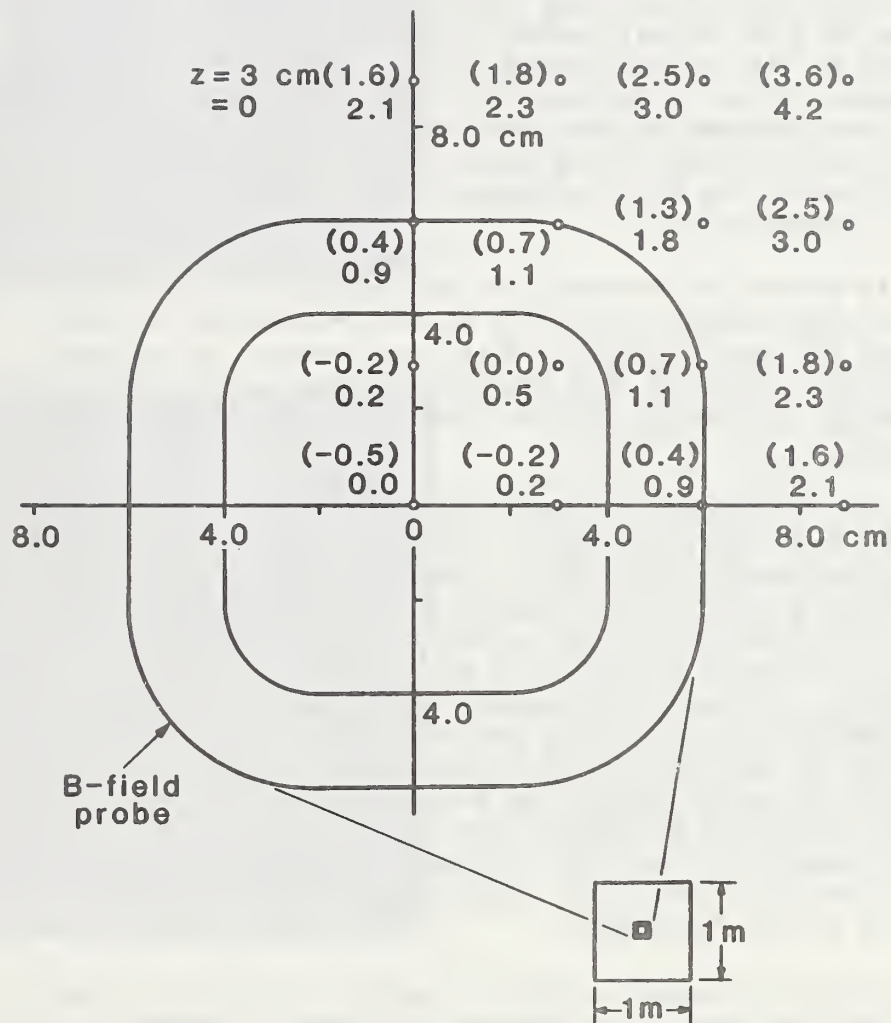
Figure 11. Percentage departure of B_z from $B_z(0,0,0)$ for positions in the plane of a square loop 1 m x 1 m, and 3 cm above or below the plane (parentheses). A scale drawing of a coil-type probe is outlined.

shown in figure 11, the calibration field is within 2% of the central value, $B_z(0,0,0)$.

4.4 Harmonic Content Measurements

To reduce the possibility of attributing biological effects that may occur at frequencies [41] other than 60 Hz to the power frequency field, the harmonic content in exposure fields should be minimized. When determining what is an acceptable level of harmonic content, it should be noted that the current induced in a biological system by a particular harmonic field component will be weighted by its harmonic number [42]. This result is suggested by the frequency dependence in the expressions for induced current, eq. (6), and emf, eq. (7) in conductors produced by electric and magnetic fields, respectively. If, for example, the exposure field contains 3% of the third harmonic, the induced current due to the third harmonic field component will be about 8.3% of the total induced current.

Possible sources of harmonics in the exposure field include harmonics in the line voltage, excessive loading of the transformer, or use of a transformer designed for applications in which the presence of harmonics is of no consequence. The use of a line conditioner in the power supply, suggested previously, can reduce the total harmonic content in the line voltage to less than 0.5%.

If the power frequency harmonic content in the exposure fields are the order of 2 to 3%, the simple fieldmeters described earlier for electric and magnetic field measurements (Sections 4.1 and 4.2) can be used with an oscilloscope to verify the presence of the harmonics in a semiquantitative fashion. This is possible because the distortion of a 60-Hz waveform is discernable visually by the presence of 6% of the third harmonic and lesser amounts of the higher order harmonics. Consequently, because the fieldmeters described previously enhance the harmonics (eq. 6 and 7), the signal from, for example, the operational amplifier of the electric field probe will reveal the presence of 2% of the 3rd harmonic and lesser amounts of the higher order harmonics in the field. Figures 12 through 14 compare pure 60-Hz waveforms with waveforms containing various amounts of the 3rd, 4th, and 5th harmonic. The distortion produced by the harmonics is seen to be a function of phase relation of the harmonic relative to the fundamental.

The waveform of magnetic fields of order 10^{-4} tesla (1 gauss), with enhanced harmonics, can usually be observed by directly connecting the coil probe to an oscilloscope.

If a quantitative measure of the harmonic content of an electric or magnetic field waveform is desired, the electrical signals can be decomposed into their harmonic components with a spectrum or waveform analyzer. However, proper accounting should be made of the weighting of each harmonic component if the field probes described above are used for such measurements.
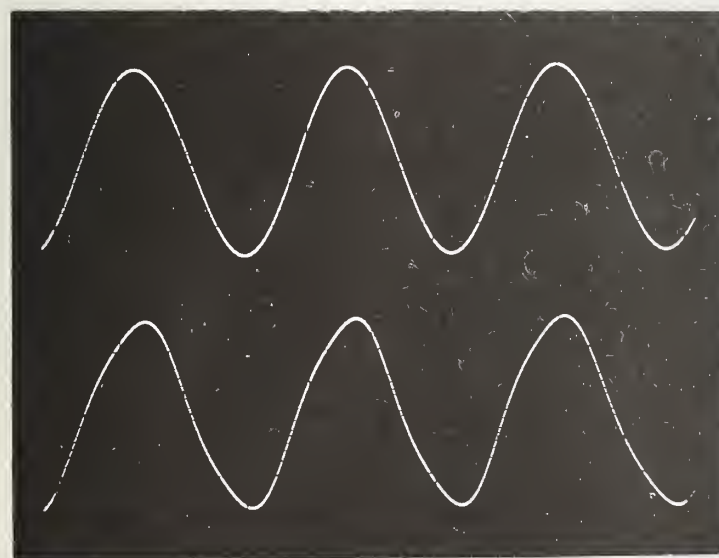
4.5 Phase Measurements

As noted earlier, the phase difference between the two magnetic field components must be 90° in order to generate a circularly polarized magnetic field. In

22
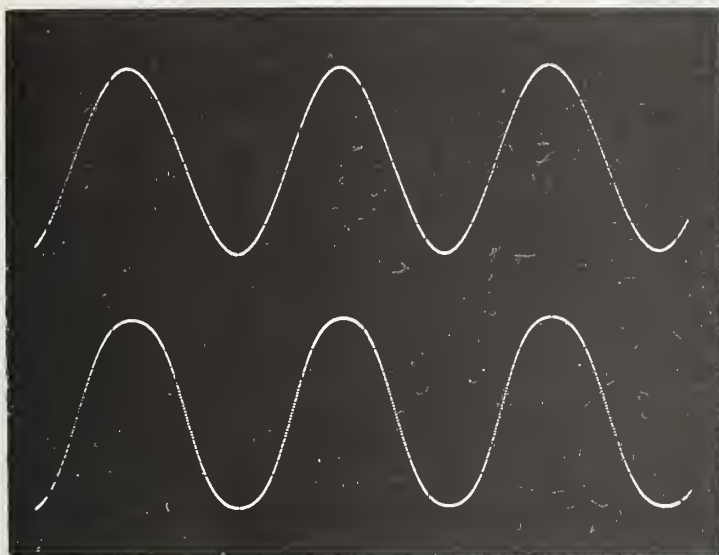
(a)
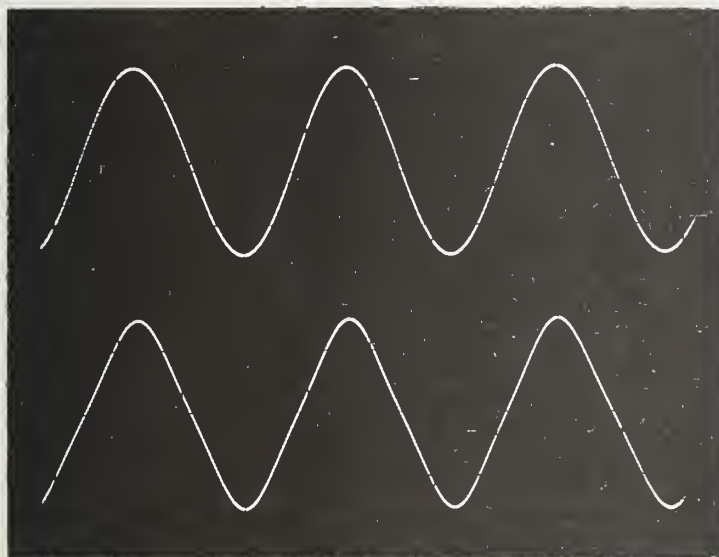
(b)

(c)

Figure 12. Effect of 3rd harmonic on sine wave: (a) sine wave (top) and sine wave combined with 6% 3rd harmonic, in phase (bottom); (b) sine wave and sine wave combined with 6% 3rd harmonic, 180° out of phase; (c) sine wave and sine wave combined with 6% 3rd harmonic, 90° out of phase. Using the probes described in the text, the waveforms with 6% 3rd harmonic would correspond to what would be observed if there was 2% 3rd harmonic in the field.
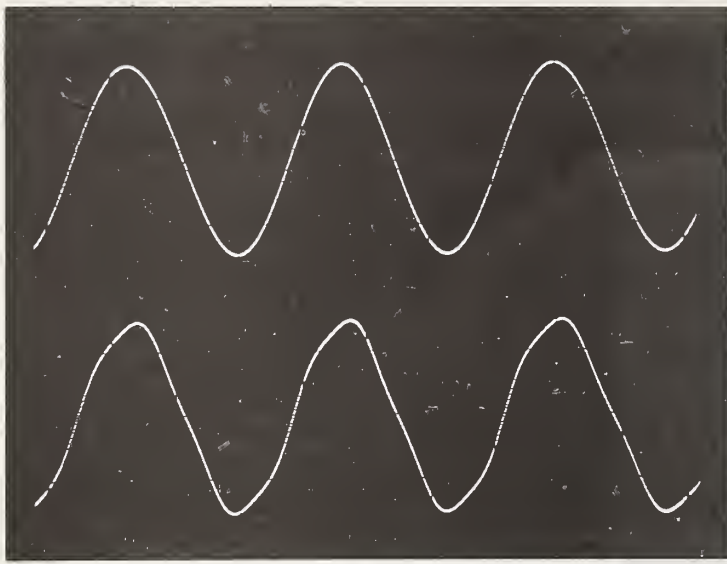
23

(a)

(b)

(c)

Figure 13. Effect of 4th harmonic on sine wave: (a) sine wave (top) and sine wave combined with 4% 4th harmonic, in phase (bottom); (b) sine wave and sine wave combined with 4% 4th harmonic, 180° out of phase; (c) sine wave and sine wave combined with 4% 4th harmonic, 90° out of phase. Using the probes described in the text, the waveforms with 4% 4th harmonic would correspond to what would be observed if there was 1% 4th harmonic in the field.
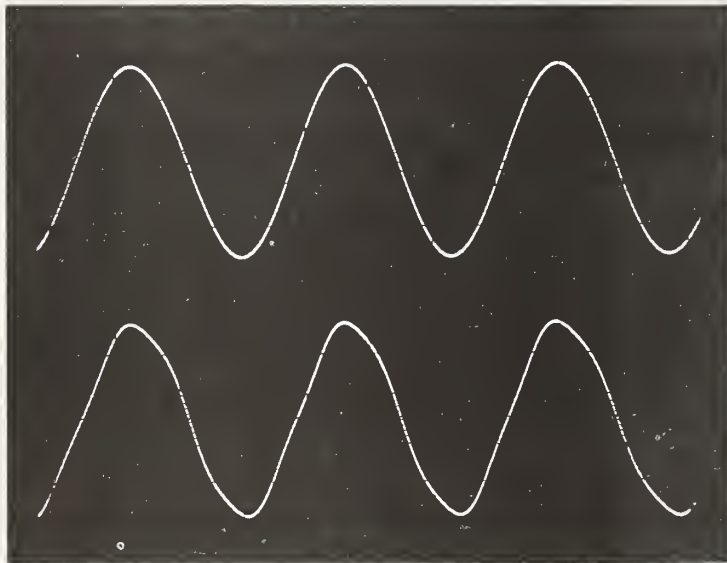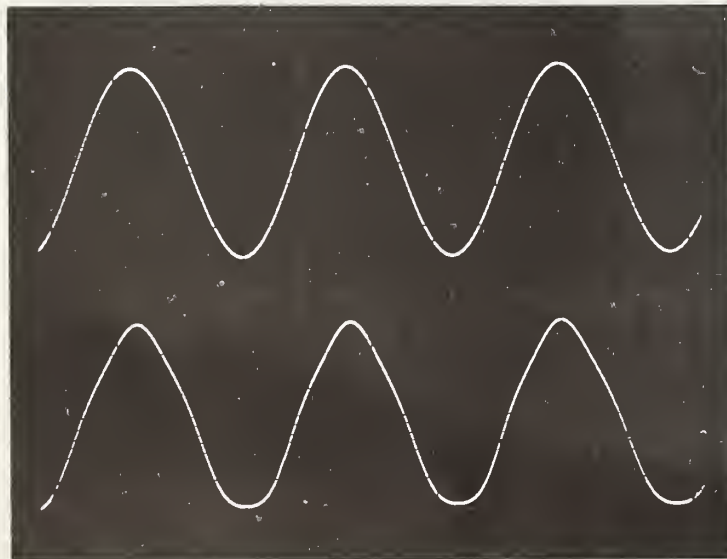
24

(a)

(b)

(c)

Figure 14. Effect of 5th harmonic on sine wave: (a) sine wave (top) and sine wave combined with 3% 5th harmonic, in phase (bottom); (b) sine wave and sine wave combined with 3% 5th harmonic, 180° out of phase, (c) sine wave and sine wave combined with 3% 5th harmonic, 90° out of phase. Using the probes described in the text, the waveforms with 3% 5th harmonic would correspond to what would be observed if there was 0.6% 5th harmonic in the field.
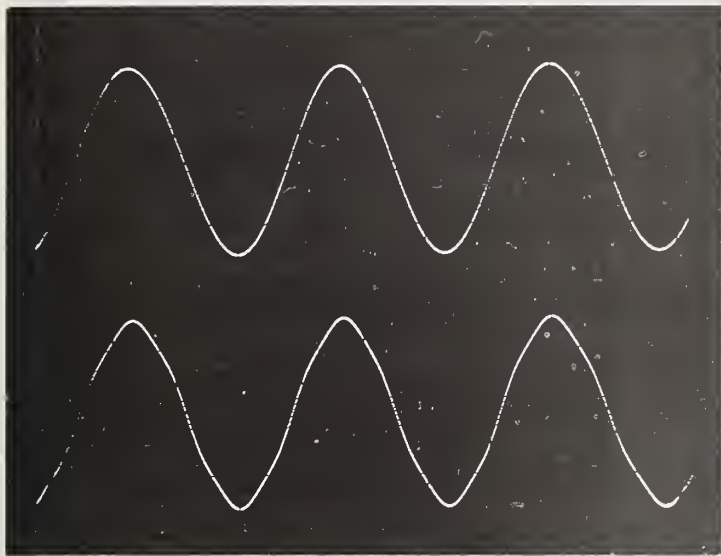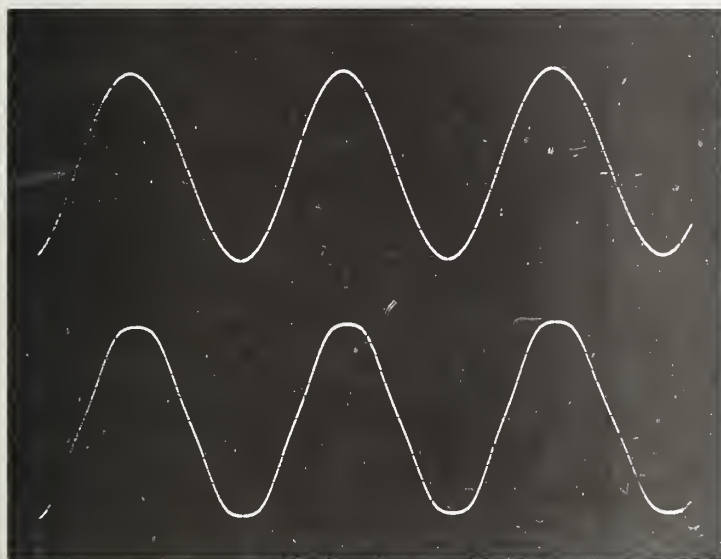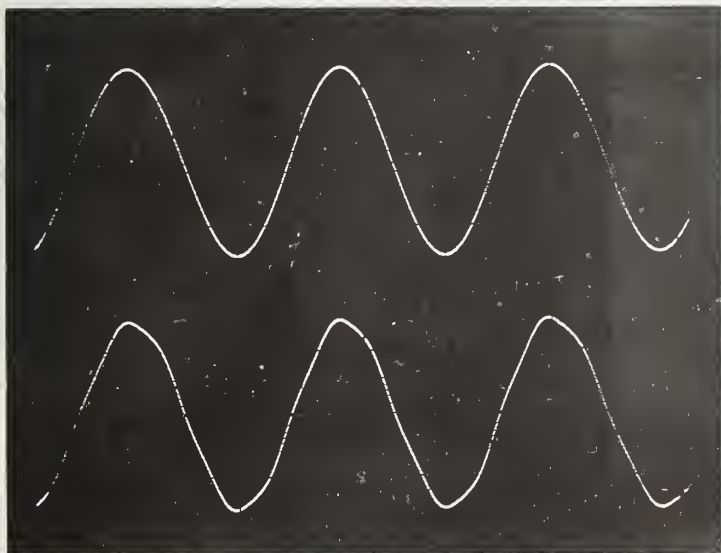
addition, the vertical magnetic field component is required to be in phase with the vertical electric field in the animal study experiments supported by the State of New York [43].

The phase relation of the magnetic field components can be determined by simultaneously observing the waveform of the currents to the two sets of coils producing the magnetic fields or by observing the magnetic field waveforms with magnetic field probes of the type described in Section 4.2 The current waveforms can be monitored by using a dual beam oscilloscope to observe the voltages across small resistances (e.g., ~1 ohm) placed in series with leads going to each set of coils. Similarly the emf's generated by the coil-type probes, aligned with the magnetic field directions, can be observed with a dual beam oscilloscope, provided that the field is great enough for the number of turns of wire in the probe. The latter measurement approach is the preferred approach because of its sensitivity to perturbations of the magnetic field in the exposure system (see below). It should be noted that the phase of the emf's will be shifted by -90° with respect to the actual magnetic field components because, from Faraday's Law, the emf is proportional to the negative derivative of the magnetic flux [44].

The ground-referenced flat probe described in Section 4.1 can be used with an oscilloscope to observe the waveform of the electric field. However, the current induced in the probe is +90° out of phase with respect to the electric field and the electronic circuit (an inverting amplifier) introduces an additional 180° phase shift. Thus, just as in the case of the emf's produced by the magnetic field probe, the signal from the disk probe-amplifier combination will be -90° out of phase with the field that produced it. In the event that both plates of the parallel plate system are energized with a center-tapped transformer (Section 3.2), the ground referenced probe can be located on a nearby ground plane.

The suggested use of an oscilloscope for the phase measurements instead of a commercially available phase meter can be justified if precise measurements of the phase relations between the various field components are not considered necessary. The uncertainties associated with the use of an oscilloscope, a readily available laboratory instrument, are less than about ±2° as can be seen in figure 15. Figure 15(a) and 15(b) show portions of two 60-Hz waveforms that are out of phase by 90°. A departure from the quadrature relation by 4.5° (i.e., one graticule division out of 40) is readily observable in figure 15(c). By amplifying one of the waveforms as shown in figures 15(b) and 15(c), greater measurement precision can be obtained. However, care should be exercised when amplifying one of the waveforms because of the possibility of introducing nonlinearities in the expanded waveform when overdriving the oscilloscope amplifier. This technique assumes that the waveforms are free of distortion and that the dual beams of the oscilloscope are triggered simultaneously. If greater precision is required commercially available phase meters can be used in place of the oscilloscope.

When the phase relations between the magnetic and electric field components are being characterized using the techniques described above, the magnetic field measurements should be performed in the region of the exposure system where the test animals will be located. Typically, this would be close to the bottom
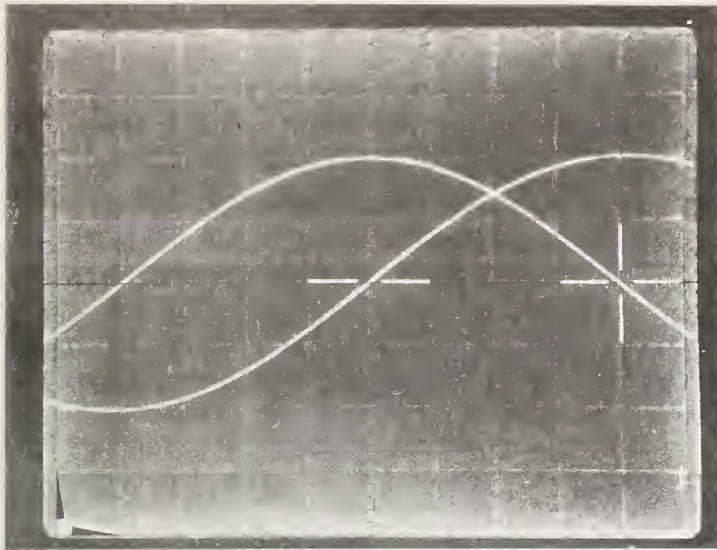
(a)
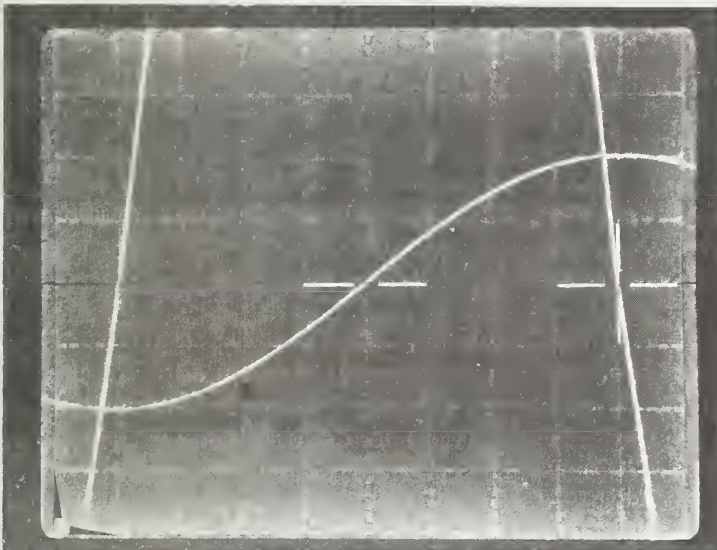
(b)
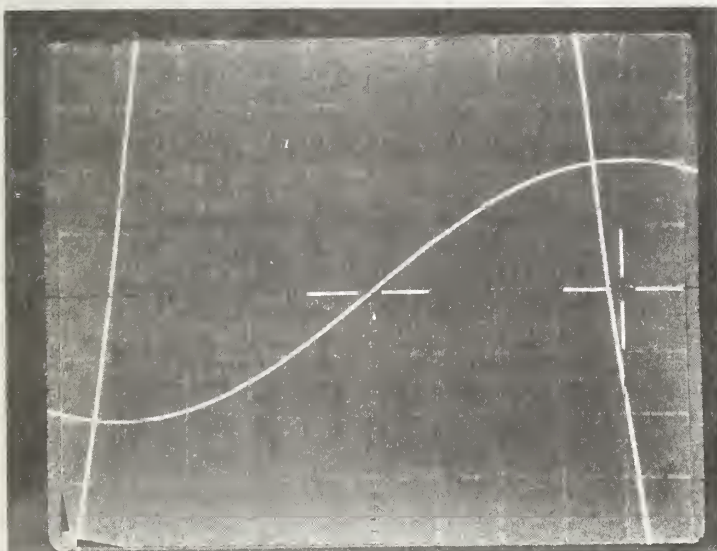
(c)

Figure 15. Determining phase
relation between waveforms with
oscilloscope.

(a) Waveforms 90° out of phase,

(b) waveforms 90° out of phase,

(c) displacement produced by
    4.5^o shift in phase is
    readily observed.

27

plate of the parallel plate system. Eddy currents in the conducting plate
(Section 3.7) can result in perturbations of the phase and magnitude of the
magnetic field which might not be apparent if the measurements are performed,
say, midway between the plates.

5. CORONA

Energizing parallel plates with the high voltages necessary to generate electric
fields that are many kV/m introduces the possibility of generating corona. One
accepted definition of corona [45] is that it is "A luminous discharge due to
ionization of the air surrounding a conductor caused by a voltage gradient
exceeding a certain critical value." In air the critical voltage gradient or
electric field near the surface of a conductor is about 3×10^6 V/m. Because
it is the electric field and not the voltage that determines the onset [46] of
corona, voltages of a few kilovolts can produce corona if applied to conductors
with inadequate insulation, sharp edges or points. Audible noise, light,
chemical products such as ozone, and radio-frequency radiation are all possible
by-products of corona. The current practice is to eliminate or minimize these
by-products because of their possible biological impact during field exposure
studies.

In general, the effects of corona can be reduced by increasing the radius of
curvature of energized and nearby grounded conductors. For example, the edges
of parallel plates can be fitted with metal tubing [19,22] and high voltage
leads can be made of metal tubing. Maximizing the distance between energized
and grounded conductors is another step that can be taken to reduce corona. In
this regard the distance between the parallel plates and magnetic field coils,
which are near ground potential, should be kept as large as practically
possible.

Qualitative methods to detect the presence of corona include listening for
audible noise, time exposure photography in a darkened room, and the use of an
am radio near the exposure system as a detector of radio frequency radiation.
Some approximate correlations have been reported between audible noise and light
and the amount of charge in corona discharges under certain conditions [47,48].
Instrumentation and measurement techniques do exist for more precise
characterizations of the charge in corona. However, the measurement procedures
are beyond the scope of this report and the interested reader is referred to
references 47 and 48 for additional information. It is noted, as in the case of
many other physical parameters associated with field exposure studies, that
there is no consensus as to what is an acceptable level of electrical discharge
activity.

6. ACKNOWLEDGMENTS

7. REFERENCES AND NOTES

1. A. O. Bulawka, W. G. Wisecup, L. A. Rosen, W. E. Feero, and F. M. Dietrich, U. S. Department of Energy 60-Hz Electric Fields Bioeffects Research, IEEE Trans. Power App. Syst., Vol. PAS-101, pp. 4432-4440, 1982.

2. R. Sander, J. Brinkmann, and B. Kuhne, Laboratory Studies on Animals and Human Beings Exposed to 50 Hz Electric and Magnetic Fields, CIGRE (International Conference on Large High Voltage Electric Systems) Paper 36-01, September, 1982.

3. J. Tuhackova and V. Cenkova, The effects of electric fields on the organism of persons in the proximity of power transmission equipment at a voltage of 400 kV or higher, electra, Vol. 83, pp. 111-117, 1982.

4. J. P. Reilly, Human Reactions to ELF Electric and Magnetic Fields - An Annotated Bibliography of Current Literature, Johns Hopkins University Applied Physics Laboratory Report JHU PPSE T-27, July 1983.

5. Biological Effects of Extremely Low Frequency Electromagnetic Fields, (Proceedings of the Eighteenth Annual Hanford Life Sciences Symposium at Richland, Washington, 1978), Editors R. D. Phillips, M. T. Gillis, W. T. Kaune, and D. D. Mahlum, available from NTIS, Springfield, Virginia 22161 as CONF-781016.

6. J. E. Bridges, Environmental Considerations Concerning the Biological Effects of Power Frequency (50 or 60 Hz) Electric Fields, IEEE Trans. Power App. Syst., Vol. PAS-97, pp. 19-32, 1978.

7. G. E. Atoian, Are There Biological and Psychological Effects Due To Extra High Voltage Installations?, IEEE Trans. Power App. Syst., Vol. PAS-97, pp. 8-18, 1978.

8. Experiments which will search for possible effects in biological systems exposed simultaneously to 60-Hz electric and magnetic fields have begun in the United States and Canada. These studies are sponsored by the State of New York Department of Health.

9. W. T. Kaune, C. H. Allen, J. L. Beamer, J. R. Decker, M. F. Gillis, R. D. Phillips, and R. L. Richardson, Biological Effects of 60-Hz Electric Fields on Miniature Swine: Exposure Facility, IEEE Trans. Power App. Syst., Vol. PAS-99, pp. 120-128, 1980.

10. C. F. Ehret, G. A. Sacher, A. Langsdorf, and R. N. Lewis, Exposure and Data-Collection Facilities for Circadian Studies of Electric Field Effects upon Behavior, Thermoregulation, and Metabolism in Small Rodents, in Reference 5.

11. R. D. Phillips, L. B. Anderson, and W. T. Kaune, Biological Effects of High Strength Electric Fields on Small Laboratory Animals, Report to the Department of Energy, 1979, available from NTIS, Springfield, Virginia 22161 as Report DOE/TIC-10084.

12. See also the references cited in References 1, 5, and 6.

13. IEEE Committee Report, Measurement of Electric and Magnetic Fields From Alternating Current Power Lines, IEEE Trans. Power App. Syst., Vol. PAS-97, pp. 1104-1114, 1978.

14. D. W. Deno, "Transmission Line Fields," IEEE Trans. Power App. Syst., Vol. PAS-95, pp. 1600-1611, 1976.

15. R. B. Adler, L. J. Chu, and R. M. Fano, Electromagnetic Energy, Transmission and Radiation (John Wiley, New York, 1960) p. 15ff.

16. Test animals have also been positioned between parallel plates during exposure to the field (Ref. 10). The surface electric field distribution and current induced in the animal will differ significantly when compared with animals in contact with one of the plates.

17. P. M. Morse and H. Feshbach, Methods of Theoretical Physics, Part II, (McGraw Hill, New York, 1953) p. 1245.

18. C. H. Shih, J. Diplacido, and B. J. Ware, Analysis of Parallel Plate Simulation of the Transmission Line Electric Field as Related to Biological Effects Laboratory Studies, IEEE Trans. Power App. Syst., Vol. PAS-96, pp. 962-968, 1977.

19. D. T. Poznaniak, J. G. Johnson, G. W. McKee, and H. B. Graves, The Design of Exposure Systems for Studying the Biological Effects of 60-Hz Electric Fields on Small Plants and Animals, in Reference 5.

20. W. T. Kaune, Interactive Effects in 60-Hz Electric-Field Exposure Systems, Bioelectromagnetics, Vol. 2, pp. 33-50, 1981.

21. F. R. Kotter and M. Misakian, AC Transmission Line Field Measurements, NBS report prepared for U. S. Department of Energy, Report No. HCP/T-6010/E1 (1977). Available from NTIS, Springfield, Virginia 22161.

22. W. T. Kaune, A Prototype System for Exposing Small Laboratory Animals to 60-Hz Vertical Electric Fields: Electrical Measurements, in Reference 5.

23. It should be noted that the enclosure shown in figure 4 was placed alongside others in the same parallel plate system to effectively raise the level of the bottom plate to that of the screen floors in the enclosures. Use of a single enclosure would result in some field enhancement at and near the surface of the screen floor.

24. C. F. Ehret, private communication. Daily cleaning of the animal enclosures is necessary for long-term exposure studies (J. J. Russell and C. F. Ehret, The Effect of Electric Field Exposure on Rat Circadian and Infradian Rhythms, Abstracts, 4th Annual Biolectromagnetics Society Meeting, Los Angeles, 1982, p. 101).

25. J. A. Creim, R. H. Lovely, W. T. Kaune, and R. D. Phillips, Attempts to Produce Taste Aversion Learning in Rats Exposed to 60-Hz Electric Fields, Bioelectromagnetics, in press.

26. See E. Weber, <u>Electromagnetic Theory</u> (Dover, New York, 1965), p. 131ff for outline of derivation.

27. S. Ramo and J. R. Whinnery, <u>Fields and Waves in Modern Radio</u> (John Wiley and Sons, New York, 1944), p. 141ff.

28. J. A. Stratton, Electromagnetic Theory (McGraw-Hill, New York, 1941), pp. 262-263.

29. H. Nazooka, Magnetic Field of Circular Current, Phil. Mag., Vol. 41, p. 377, 1921.

30. R. J. Caola, Jr., D. W. Deno, V.S.W. Dymek, Measurements of Electric and Magnetic Fields In and Around Homes Near a 500 kV Transmission Line, Paper 83WM 164-1 presented at the IEEE Power Engineering Society Meeting, Jan. 30-Feb. 4, 1983.

31. D. R. Corson and P. Lorrain, <u>Introduction to Electromagnetic Fields and Waves</u> (W. H. Freeman, San Francisco 1962) p. 285ff.

32. M. A. Plonus, <u>Applied Electromagnetics</u> (McGraw-Hill, New York 1978) pp. 398-400.

33. H. D. Cohen and C. Graham, Human Exposure Facility for Double-Blind Testing of 60-Hz Electric and Magnetic Fields. Abstracts, 5th Annual Biolectromagnetics Society Meeting, Boulder, Colorado, 1983, p. 81.

34. For a brief introduction to the phenomena of ferromagnetism, paramagnetism, and diamagnetism, see for example D. Halliday and R. Resnick, <u>Physics, Parts I and II</u> (J. Wiley, New York 1966) Chapt. 37.

35. It is noted that the disk probe can be fabricated from other materials and that it may be necessary to introduce a small amount of capacitance in the feedback circuit of the operational amplifier circuit to avoid oscillations. To minimize attenuation of signals due to power frequency harmonics which may be present in the electric field (see Section 4.4) the capacitance should be kept as small as possible.

36. S. Stern, V. G. Laties, C. V. Stancampiano, C. Cox, and J. O. de Lorge, Behavioral Detection of 60-Hz Electric Fields by Rats, Bioelectromagnetics, Vol. 4, pp. 215-247, 1983.

37. R. J. Spiegel, D. R. Kerns, E. H. Cooper, and E. L. Bronaugh, A Small Accurate, Optically Isolated Electric Field Probe, IEEE Publ. No. A79 507-5, 1979.

38. Y. Hamasaki, H. Gotoh, M. Katoh, and S. Takeuchi, OPSEF: An Optical Sensor for Measurement of High Electric Field Intensity, Electronics Letters, Vol. 16, pp. 406-407, 1980.

39. M. Misakian, F. R. Kotter, and R. L. Kahler, Miniature ELF electric field probe, Rev. Sci. Instrum. Vol. 49, pp. 933-935, 1978.

40. IEEE Recommended Practices for Measurement of Electric and Magnetic Fields from AC Power Lines, IEEE Std 644-1979 (IEEE, Inc., New York 1979) p. 13.

41. The frequencies considered here are restricted to the power frequency harmonics. Characterization of radio frequency fields are beyond the scope of this report.

42. W. T. Kaune and M. L. Gillis, General Properties of the Interaction Between Animals and ELF Electric Fields, Bioelectromagnetics, Vol. 2, pp. 1-11, 1981.

43. For in vitro experiments, the horizontal magnetic field must be in phase with the vertical electric field in air.

44. See Ref. 34, Chapter 35.

45. IEEE Standard Dictionary of Electrical and Electronic Terms, IEEE Std. 100-1977 (IEEE, Inc. New York, 1977).

46. The "onset" of corona must be described in terms of the sensitivity of the instrumentation used for the measurements. For example, it is possible, under controlled conditions, to measure the amount of charge in an avalanche associated with a corona discharge as a function of voltage applied to the conductor. It is normal to define the "onset voltage" of the corona as the voltage at which discharges containing the minimum amount of charge that can be detected, say 1 pC, as the onset voltage. Thus, there will be electrical discharges at lower voltages and with smaller amounts of charge per avalanche. See R. J. Van Brunt and M. Misakian, Mechanisms for Inception of DC and 60-Hz AC Corona in SF_6, IEEE Trans. Electrical Insulation, Vol. EI-17, pp. 106-120, 1982 for discussion of corona inception in a point-plane electrode system.

47. R. Bartnikas and E. J. McMahon, eds., Engineering Dielectrics Volume 1, Corona Measurements and Interpretation, ASTM Special Technical Publication 669, American Society for Testing and Materials, 1979.

48. F. H. Kreuger, Discharge Detection in High Voltage Equipment, (American Elsevier Publishing Co., New York, 1964).

8. APPENDIX

Theory for measurement of the electric field strength at points away from conducting surfaces and the description of a miniature electric field probe suitable for field strength measurements between parallel plates are presented here. While the miniature probe is less convenient to use compared to probes with fiber-optic links [37,38], its size, sensitivity, and relatively low cost of fabrication may justify its consideration if measurements of the field strength between parallel plates are of interest. The operational amplifiers in the detector (Fig. 4, Appendix) can be replaced by more modern components which require less power and the power supply can be replaced by two 9-volt batteries.

Miniature ELF electric field probe

Martin Misakian, F. Ralph Kotter, and Richard L. Kahler

Electrosystems Division, National Bureau of Standards, Washington, D.C. 20234

(Received 3 October 1977; in final form, 10 March 1978)

A miniature ac electric field probe having direct electrical connections with its battery-operated electronics is described. Because its small size introduces little field perturbation, fields generated by relatively small electrode structures in laboratory environments can readily be characterized.

INTRODUCTION

A miniature electric field (E field) probe which is well removed from its battery-operated electronics with wires has recently been developed as part of a program to evaluate field measurement procedures and instrumentation used under high-voltage ac transmission lines. Because its small size introduces little field perturbation, the probe has been successfully employed to obtain 60-Hz E-field "maps" between laboratory parallel-plate structures used for field meter calibrations. It has also been used in a similar fashion to measure fields between small parallel plates used for biological experiments. Since calculation of these fields is complicated by the presence of nearby ground planes (e.g., walls, floor) and, in the case of biological studies, animal enclosures, food, and water, the probe measurements provide an alternative and perhaps more accurate approach for characterizing the E field in a laboratory environment.

A search of the literature indicates that this is perhaps the first ac E-field probe, operable above the ground plane, having direct electrical connections between the field sensing elements and electronics. Considerably more complex devices have been developed which employ glass fiber optics to couple the probe with its signal processing circuits.[1]

I. THEORY

The theory of operation is readily developed by considering a conducting sphere of radius a and electric potential $V \sin(\omega t + \phi)$ in a quasistatic uniform field $E = E_0 \sin\omega t$ as shown in Fig. 1(a). The perturbed electric field is given in spherical coordinates by[2]

$$\mathbf{E} = -\hat{a}_r\{[K \sin\omega t - V \sin(\omega t + \phi)]ar^{-2}$$
$$+ E_0[1 + 2(a/r)^3] \cos\theta \, \sin\omega t\}$$
$$+ \hat{a}_\theta E_0[1 - (a/r)^3] \sin\theta \, \sin\omega t, \quad (1)$$

where $K \sin\omega t$ is the space potential at $z = 0$ prior to the introduction of the sphere. At the sphere's surface ($r = a$), the magnitude of $\mathbf{E}$ is

$$E_s = [K \sin\omega t - V \sin(\omega t + \phi)]a^{-1} + 3E_0 \sin\omega t \cos\theta, \quad (2)$$

and the surface charge density σ is given by $\epsilon_0 E_s$, where ϵ_0 is the electric permittivity of space.

The total induced charge on the top hemisphere is found from the surface integral

$$Q = \int_0^{\pi/2} \int_0^{2\pi} \sigma a^2 \sin\theta \, d\theta d\phi$$
$$= C_1[K \sin\omega t - V \sin(\omega t + \phi)] + C_2 E_0 \sin\omega t. \quad (3)$$

Here C_1 and C_2 are constants which depend on conductor geometry. The induced current is just

$$I_0 = \frac{dQ}{dt}$$
$$= \omega C_1[K \cos\omega t - V \cos(\omega t + \phi)]$$
$$+ \omega C_2 E_0 \cos\omega t. \quad (4)$$

Less symmetric conductor geometries (e.g., a rectangular box) will lead to equations of the same form for Q and I_0.

If the sphere's potential is set equal to the ambient space potential, $K \sin\omega t$, it can be seen from Eqs. (3) and (4) that measurement of the induced charge or current permits the determination of E_0 to within a known constant. This constant can be found for other surface geometries by calibration. It should also be noted that the potential of the now electrically "floating" sphere will be the same as the space potential of the equatorial plane, $\theta = \pi/2$.

The above matching of electric potentials is achieved for large commercial 60-Hz E-field meters (used under high-voltage transmission lines) by housing the battery operated electronics and analog meter between the sensing electrodes ("hemispheres") and supporting the device in the E field with a long dielectric rod.[3] The
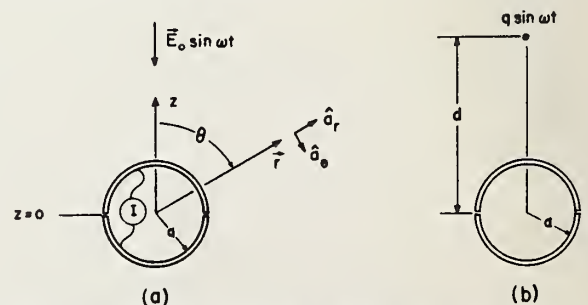

FIG. 1. Geometries for calculating induced charge and current for uniform (a) and nonuniform (b) quasistatic fields.
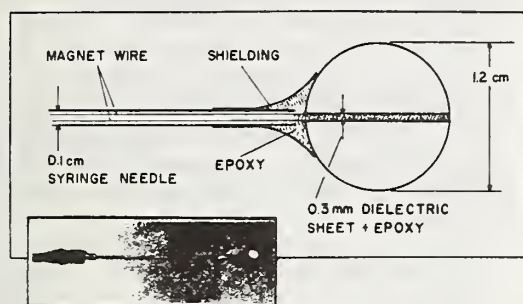
34

FIG. 2. Schematic view of electric field probe. The wires are connected to the aluminum sensing elements with conducting adhesive and the elements are joined with epoxy. A thin dielectric sheet separates the hemispheres. The lead wires are fully shielded with a 9.5-cm-long syringe needle handle and metal foil tape.

miniature E-field probe described in the next section also "floats" electrically but the potential is set using a potentiometer.[4]

While the above theory has considered a uniform field, the usefulness of the probe for measuring highly non-uniform fields is also expected. The quasistatic field near a point charge, $q \sin \omega t$, is used to demonstrate this. An electrically isolated spherical E-field probe is now considered aligned along a field line at a distance d from q as shown in Fig. 1(b). The induced current in the top hemisphere can be shown to equal[5]

$$I_q = \omega C_2 E \cos \omega t$$
$$\times \left[1 - \frac{7}{12} \left(\frac{a}{d} \right)^2 + \frac{11}{24} \left(\frac{a}{d} \right)^4 - \ldots \right], \quad (5)$$

where

$$E = (1/4\pi\epsilon_0)q/d^2.$$

Comparison of Eqs. (4) and (5) shows that the induced current for the nonuniform field case is the same as that produced by a uniform field of amplitude $E_0 = q/4\pi\epsilon_0 d^2$ if the terms in (a/d) can be neglected. Thus the induced current at a point in the highly nonuniform field produced by a point charge is nearly the same as that produced by a uniform field of equal magnitude if d is sufficiently large. For example, if $a/d = 0.1$, the difference in induced current or charge (i.e., E-field measurement) produced by a uniform and highly non-uniform field is less than 1%. In this case, the field changes in magnitude over the dimensions of the sphere by $|\Delta E/E| \approx 4(a/d) = 0.4$ (40%)! The discussion in this section assumes that the charges producing the field are not perturbed by the presence of the conducting sphere.

II. APPARATUS AND METHOD

A schematic view of the miniature field probe is given in Fig. 2. The field sensing surfaces are electrically isolated portions of an aluminum sphere 1.2 cm in diameter. Small diameter (~0.1 mm) magnet wires provide the connections between a shielded extension cable and the sensing surfaces through a syringe needle shield which also serves as a handle for positioning the probe (Fig. 2 inset).

The probe and its associated battery operated electronics are shown greatly simplified in Fig. 3. A 60-Hz calibration E field is generated with parallel plates and the induced charge on the hemispherical sensing plates is measured with a differential amplifier that is housed in an electrically biased chassis box. This bias is adjusted to be the space potential in the equatorial plane near the sphere using the space potential probe–ammeter[6]–potentiometer combination. A voltage null indicates when the bias is appropriately set. No serious difficulty was encountered in achieving voltage nulls when the lead wire from the potentiometer was approximately 2 m long. The condition $\phi \neq 0$ [Eq. (4)] can develop, however, when very long connecting wires are used because of stray capacitance. The phase shift must be eliminated with appropriate circuitry (e.g., an RC network) to achieve a null.

The handle of the field probe should be aligned with an equipotential surface. In uniform field, the equatorial plane of the probe, shown in the inset of Fig. 3, will then coincide with this surface. The space potential probe consists of a shielded (aluminum foil) subminiature coaxial cable ~1.5 mm in diameter with approximately 2 mm of insulated but unshielded center conductor at its sensing end. The potential probe is brought near the field probe along the equatorial plane. The field probe shown in the inset of Fig. 3 has quarter-sphere sensing elements which permit measurement of two orthogonal field components without reorienting the probe. A switching arrangement indicated in Fig. 4 connects different pairs of elements for each measurement.

Figure 4 provides a more detailed view of the field probe electronics. Because of the small current flow between the + input and chassis (less than ~10 nA at 10 kV/m), the + input will effectively be at the chassis bias potential which is set with the potentiometer. Thus both hemispherical surfaces as well as the shielding will be set to the appropriate potential when a null is
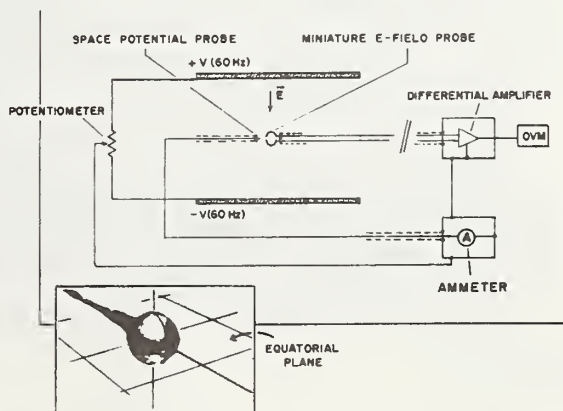

FIG. 3. Simplified schematic view of field probe and associated electronics. A space potential probe is used in conjunction with a potentiometer to set the field probe potential and shielding to the value in the equatorial plane. The sphere is electrically "floating" at the appropriate potential when the voltmeter is nulled.
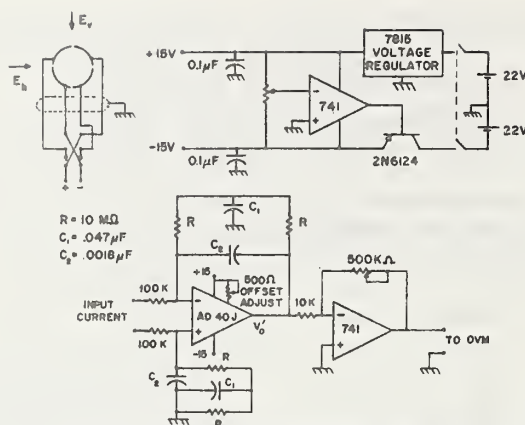
FIG. 4. Field probe amplifier and power supply. The induced current is integrated to obtain a measure of the induced charge or E field when the chassis potential is appropriately set. The AD 40J operational amplifier is employed because of its high input impedance and low bias currents.[10] The transfer function of the first stage is independent of frequency for 60 Hz and power frequency harmonics. A switching arrangement ties together different pairs of sensing elements to permit measurement of two orthogonal components of the E field.

achieved.[7] The space potential probe is removed during field measurements.

Capacitive feedback has been used in the first-stage amplifier in order to integrate the input current [Eq. (4)] and develop a frequency-independent output voltage V_0' proportional to induced charge [Eq. (3)]. A second stage of amplification follows and the rms value of the output is read with a battery-operated (rectified) average-sensing digital voltmeter (DVM). Because of the average sensing rms feature of the DVM, measurement of charge to determine E rather than current will lead to smaller errors if there are harmonic components in the E field.[8] This occurs because the charge induced by a given E-field harmonic field component is not weighted by its harmonic number; harmonic components of current are so exaggerated however.

The probe is calibrated and tested in a uniform field produced with parallel plates $1 \times 1 \times 0.5$-m separation and energized using a center tapped current limited transformer. The expected constant vertical E field is observed along the vertical axis. Vertical ground planes brought to within 0.25 m of the plate edges do not measurably affect this profile. Significant field perturbation will occur, however, if the bottom plate of the apparatus is grounded. Perturbation of the surface charge density when the probe is within 5 cm of a plate surface leads to a measurement error of less than 1%. The sensitivity of the electronics shown in Fig. 4 is adequate for measuring fields as low as 2 kV/m.

The theoretical expectation that highly nonuniform

fields can be measured with little error when the probe is aligned with the field direction was not directly tested with the miniature probe. However, an investigation using large commercial field meters (~19 cm vertical dimension) has confirmed within experimental uncertainty ($\leqslant 5\%$) that field meters calibrated to measure uniform fields can successfully be used in fields which change by ~30% in magnitude over the probe dimensions.[9]

ACKNOWLEDGMENT

[1] L. Wilhelmy, Elektrotech. Z. A **94**, 441 (1973); A. R. Valentino, Proc. IEEE International Symposium on Electromagnetic Compatibility (July 1972), p. 265 (unpublished), available as IIT Research Institute Report No. AD 742128 from NTIS, Springfield, VA 22161. Since the time the present manuscript was submitted, we have learned that a probe similar to the NBS miniature probe has been developed at Ohio State University [see S. A. Sebo, report to Electric Power Research Institute, EL-632, Vol. 1, Res. Proj. 753, pp. 5–13. January 1978 (unpublished)].
[2] P. Moon and D. E. Spencer, *Field Theory for Engineers* (Van Nostrand, Princeton, NJ, 1961), p. 225 ff.
[3] A forerunner of these electrically isolated field meters was a device referenced to ground ($V = 0$) and used for a number of years to measure electric fields above the ground plane [C. J. Miller, IEEE Trans. Power App. Syst. **PAS-86**, 493 (1967)]. Under these conditions the first term in Eq. (4) does not vanish and erroneous measurements are obtained.
[4] The idea of electrically adjusting the probe potential to match the space potential for accurate field measurements is not new. It has been used for many years to measure the potential gradient of the earth's atmosphere. See, for example, M. Smiddy and J. A. Chalmers, J. Atmosph. Terr. Phys. **12**, 206 (1958) and S. Gathman, Rev. Sci. Instrum. **39**, 43 (1968).
[5] This result is given without derivation in the CIGRE article "Electrical Field Measurement in the Vicinity of HV Equipment and Assessment of Its Bio-Physiological Perturbing Effects," by C. Mihaileanu *et al.* (CIGRE Paper 36-08, 1976, Paris, France). It can be derived by considering an uncharged conducting sphere in the field of a point charge and using the method of images.
[6] Model 100-10 electric field meter accessory, Electric Field Measurements Company, West Stockbridge, MA. The identification of commercial equipment and their sources is made to adequately describe the experimental results. In no case does this identification imply recommendation by the National Bureau of Standards, nor does it imply that the device is the best available.
[7] In a uniform E field, the unperturbed space potential, ϕ_0, at $z = 0$ (Fig. 1) will be equal to the potential value in the equatorial plane after an electrically isolated sphere is introduced into the field. In the present case, the sphere is initially at some arbitrary potential $\phi \neq \phi_0$ and the equatorial plane near the sphere will not be at the appropriate potential ϕ_0. As the voltage difference between the sphere and space potential probe is reduced, however, the potential surfaces near the sphere approach the geometry which is characteristic for an electrically isolated sphere.
[8] M. R. Negrete, IEEE WESCON Tech. Papers 9, pt. 6 (1965).
[9] F. R. Kotter and M. Misakian, NBS report prepared for U.S. Department of Energy, Report No. HCP/T-6010/E1 (1977) (unpublished). Available from NTIS, Springfield, VA 22161.
[10] The disclaimer in Ref. 6 again applies.

36

11. ABSTRACT (A 200-word or less factual summary of most significant information. If document includes a significant bibliography or literature survey, mention it here)

This report presents material which is intended to provide assistance in the measurement of a number of electrical parameters that are of importance during bioeffects research involving 60-Hz electric and magnetic fields. The parameters that are considered are the electric field strength E, the magnetic induction or flux density B, field uniformity, harmonic content, phase relations between field components, and corona. Descriptions of the fields and methods for their laboratory generation are surveyed. The text is purposely elementary with references provided to aid the interested reader in obtaining a fuller understanding of many of the topics. It is shown that using relatively simple instrumentation, it is possible to characterize reasonably well the electric and magnetic fields used in animal exposure studies.

NBS TECHNICAL PUBLICATIONS

PERIODICALS

JOURNAL OF RESEARCH—The Journal of Research of the National Bureau of Standards reports NBS research and development in those disciplines of the physical and engineering sciences in which the Bureau is active. These include physics, chemistry, engineering, mathematics, and computer sciences. Papers cover a broad range of subjects, with major emphasis on measurement methodology and the basic technology underlying standardization. Also included from time to time are survey articles on topics closely related to the Bureau's technical and scientific programs. As a special service to subscribers each issue contains complete citations to all recent Bureau publications in both NBS and non-NBS media. Issued six times a year. Annual subscription: domestic $18; foreign $22.50. Single copy, $5.50 domestic; $6.90 foreign.

NONPERIODICALS

Monographs—Major contributions to the technical literature on various subjects related to the Bureau's scientific and technical activities.

Handbooks—Recommended codes of engineering and industrial practice (including safety codes) developed in cooperation with interested industries, professional organizations, and regulatory bodies.

Special Publications—Include proceedings of conferences sponsored by NBS, NBS annual reports, and other special publications appropriate to this grouping such as wall charts, pocket cards, and bibliographies.

Applied Mathematics Series—Mathematical tables, manuals, and studies of special interest to physicists, engineers, chemists, biologists, mathematicians, computer programmers, and others engaged in scientific and technical work.

National Standard Reference Data Series—Provides quantitative data on the physical and chemical properties of materials, compiled from the world's literature and critically evaluated. Developed under a worldwide program coordinated by NBS under the authority of the National Standard Data Act (Public Law 90-396).

NOTE: The principal publication outlet for the foregoing data is the Journal of Physical and Chemical Reference Data (JPCRD) published quarterly for NBS by the American Chemical Society (ACS) and the American Institute of Physics (AIP). Subscriptions, reprints, and supplements available from ACS, 1155 Sixteenth St., NW, Washington, DC 20056.

Building Science Series—Disseminates technical information developed at the Bureau on building materials, components, systems, and whole structures. The series presents research results, test methods, and performance criteria related to the structural and environmental functions and the durability and safety characteristics of building elements and systems.

Technical Notes—Studies or reports which are complete in themselves but restrictive in their treatment of a subject. Analogous to monographs but not so comprehensive in scope or definitive in treatment of the subject area. Often serve as a vehicle for final reports of work performed at NBS under the sponsorship of other government agencies.

Voluntary Product Standards—Developed under procedures published by the Department of Commerce in Part 10, Title 15, of the Code of Federal Regulations. The standards establish nationally recognized requirements for products, and provide all concerned interests with a basis for common understanding of the characteristics of the products. NBS administers this program as a supplement to the activities of the private sector standardizing organizations.

Consumer Information Series—Practical information, based on NBS research and experience, covering areas of interest to the consumer. Easily understandable language and illustrations provide useful background knowledge for shopping in today's technological marketplace.

Order the above NBS publications from: Superintendent of Documents, Government Printing Office, Washington, DC 20402.

Order the following NBS publications—FIPS and NBSIR's—from the National Technical Information Service, Springfield, VA 22161.

Federal Information Processing Standards Publications (FIPS PUB)—Publications in this series collectively constitute the Federal Information Processing Standards Register. The Register serves as the official source of information in the Federal Government regarding standards issued by NBS pursuant to the Federal Property and Administrative Services Act of 1949 as amended, Public Law 89-306 (79 Stat. 1127), and as implemented by Executive Order 11717 (38 FR 12315, dated May 11, 1973) and Part 6 of Title 15 CFR (Code of Federal Regulations).

NBS Interagency Reports (NBSIR)—A special series of interim or final reports on work performed by NBS for outside sponsors (both government and non-government). In general, initial distribution is handled by the sponsor; public distribution is by the National Technical Information Service, Springfield, VA 22161, in paper copy or microfiche form.